

Sandro Mereghetti

The strongest cosmic magnets: Soft Gamma-ray Repeaters and Anomalous X-ray Pulsars

Received: date

Abstract Two classes of X-ray pulsars, the Anomalous X-ray Pulsars and the Soft Gamma-ray Repeaters, have been recognized in the last decade as the most promising candidates for being magnetars: isolated neutron stars powered by magnetic energy. I review the observational properties of these objects, focussing on the most recent results, and their interpretation in the magnetar model. Alternative explanations, in particular those based on accretion from residual disks, are also considered. The possible relations between these sources and other classes of neutron stars and astrophysical objects are also discussed.

Keywords First keyword · Second keyword · More

1 Introduction

Magnetars are neutron stars with magnetic fields much larger than the quantum critical value $B_{QED} = \frac{m^2 c^3}{\hbar e} = 4.4 \times 10^{13}$ G, at which the energy between Landau levels of electrons equals their rest mass. Their magnetic fields are at least 100-1000 times stronger than those of the typical neutron stars observed as radio pulsars powered by the loss of rotational energy, or shining in X-rays thanks to the accretion of matter from binary companion stars. Magnetic field is the ultimate energy source of all the observed emission from magnetars [236; 237].

Magnetars have attracted increasing attention in the last decade, being extremely interesting objects, both from the physical and astronomical point of view. They allow us to observe and study several phenomena taking place

S. Mereghetti
INAF - IASF Milano
via E. Bassini 15, I-20133 Milano, Italy
E-mail: sandro@iasf-milano.inaf.it

in magnetic field conditions not available elsewhere (see, e.g., [109]). Their astrophysical importance is due to the fact that they broadened our views of how neutron stars are formed and evolve. Together with other new classes of neutron stars observed through the whole electromagnetic spectrum, they indicate that the classical radio pulsars discovered forty years ago are just one of the diverse manifestations of neutron stars.

Magnetars are historically divided in two classes of neutron stars that were independently discovered through different manifestations of their high-energy emission: the Soft Gamma-ray Repeaters (SGRs) and the Anomalous X-ray Pulsars (AXPs). SGRs were discovered through the detection of short bursts in the hard X-ray/soft gamma-ray range, and initially considered as a subclass of gamma-ray bursts [165; 7]. AXPs were first detected in the soft X-ray range (<10 keV) and thought to belong to the population of galactic accreting binaries; only as more X-ray data accumulated, and deeper optical/IR searches excluded the presence of bright companion stars, their peculiar properties started to appear, leading to their classification as a separate class of pulsars [190]. Observations performed over the last few years led to new discoveries pointing out many similarities between these two classes of objects [262]. Thus, the magnetar model initially developed to explain the extreme properties of the SGRs, difficult to interpret in other models [49], was applied also to the AXPs [237].

The main observational properties that led to the recognition of the AXPs as a homogenous class, different from the more common accretion-powered pulsars in massive X-ray binaries, were the following [190; 183]:

- (a) lack of evidence of binary companions
- (b) luminosity larger than the spin-down power
- (c) spin period in the 5-12 s range
- (d) secular spin-down on timescales of 10^3 - 10^5 years
- (e) no (or very small) long term variability
- (f) soft X-ray spectrum
- (g) absence of radio emission
- (h) (in some cases) association with supernova remnants

When the persistent X-ray counterparts of SGRs were found, it was apparent that they shared many of these properties: they showed luminosities, periods and period derivatives similar to the AXPs, but had generally harder spectra. Possible associations with SNRs were reported for all the four confirmed SGRs.

After more of ten years of extensive observations in many wavelengths, most of the above properties have been consolidated on the basis of better data, but a few of them (e.g. (e) and (g)), sometimes unexpectedly, have not been confirmed:

(a) and (b) – these two properties remain prerequisite characteristics to exclude more conventional explanations for newly discovered X-ray pulsars. Much progress has been done in the search for optical/IR counterparts (sect. 5.1) and the resulting faintness of the candidates has confirmed that standard binary systems powered by accretion from a companion are excluded.

(*c*) and (*d*) – the characteristic P and \dot{P} values of these objects have been confirmed. The reason for the narrow distribution of period values is not obvious (sect. 4.1). The timing signatures have provided a wealth of important information, through the measurement of noise and glitches (sect. 4.2), as well as through the observation of quasi-periodic oscillations (QPOs) and other effects during the SGR giant flares (sect. 3.2).

(*e*) – one of the most interesting results of the observations carried out in the last few years is that, at variance with most manifestations of isolated neutron stars powered by rotational energy or residual heat, the magnetically-powered X-ray emission from AXPs and SGRs is variable on different time scales (sect. 3.3). Long term flux variations have now been observed in virtually all objects for which accurate measurements are available. In addition, there are a few remarkable cases of transient magnetars, spanning a range of 2-3 orders of magnitude in luminosity (sect. 3.4). On the shortest time scales, the rapid bursts that were the defining characteristic of SGRs have now been seen in also in most AXPs, although with smaller peak luminosity and possibly slightly different properties (sect. 3.1). The spectacular flares seen in SGRs (sect. 3.2) were traditionally classified in giant and intermediate, but as more events are found, including those seen in AXPs, it seems that they rather span a continuum of intensities. A coherent picture relating all these variability phenomena has not emerged yet. In several cases there is evidence that the luminosity variations on medium and long term are associated to sudden events like bursts or glitches (sect. 4.2). On the other hand, there are also long term variations apparently unrelated to such events, although the sparse coverage of the observations does not allow to draw firm conclusions.

(*f*) – the softness of AXP spectra below 10 keV has been confirmed, but observations with the INTEGRAL satellite above 20 keV have unexpectedly shown the presence of a significant flux of hard X-rays in the persistent (i.e. not bursting) emission from several AXPs and SGRs (sect. 2.4). This discovery is particularly important since it turns out that the bolometric output from these objects can be dominated by non-thermal magnetospheric emission.

(*g*) – another rather unexpected result is the discovery of pulsed radio emission from two AXPs (sect. 5.2). This property seems to be a prerogative of transient magnetars. The presence of pulsed radio emission, besides its intrinsic interest, provides a new important diagnostic tool for several other aspects of the study of magnetars: it allows to derive independent distance estimates and very precise position determinations, possibly leading to proper motion measurements. Furthermore, pulse timing measurements in the radio band can be carried with a higher precision and on shorter time scales than in X-rays, thus offering a better tool to study glitches and torque variations.

(*h*) – the association with SNRs is robust in two or three objects, but not considered significant in several other cases that were proposed in the past.

Table 1 lists all the known magnetars¹ and candidate magnetars. Compared to a few years ago, when these objects were studied mostly in X-rays, it is striking to see the important role now played by multi-wavelength observations.

¹ I will use the term magnetar when referring to both AXPs and SGRs.

Several reviews on magnetars are already available [182; 262; 145], therefore I will concentrate here mainly on the more recent developments in this very dynamical field. In the next three sections I describe the observational properties of AXPs and SGRs. The main concepts of the magnetar model are then discussed (sect. 6), while alternative models are presented in section 7. In section 8 I discuss the possible relations between magnetars and other classes of astrophysical objects. Some prospects for future observations are given in the concluding section.

Table 1 Multiwavelength emission from AXPs and SGRs

Name ^(a)	Hard X-rays ^(b) (>10 keV)	Soft X-rays ^(b) (<10 keV)	Optical ^(b)	IR ^(b)	Radio ^(b)	Distance (kpc)	Location
Anomalous X-ray Pulsars							
CXOU J0100-72 [163]	-	P [163]	-	-	-	61	SMC
4U 0142+61 [190]	P [42]	P [138]	P [150]	D [121; 252]	-	3.6 [51]	
1E 1048-59 [190]	D [169]	P [222]	-	D [251; 136]	-	9 [51]	
1E 1547-54 [86]	-	P,T [107]	-	-	P [22]	9 [22]	SNR G327.24-0.13
CXOU J1647-45 [195]	-	P,T [196; 133]	-	-	-	3.9 [154]	Massive Star Cluster Westerlund 1
1RXS J1708-40 [227]	P [160; 97]	P [227]	-	D? [53; 233]	-	3.8 [51]	
XTE J1810-197 [125]	-	P,T [125; 92]	-	D [139]	P [105; 23]	3.1 [51]	
1E 1841-045 [244]	P [161; 194]	P [244]	-	D? [233]	-	8.5 [167]	SNR Kes 73
AX J1845-02 ^(c) [241]	-	P,T [241]	-	-	-	8.5 [241]	SNR G29.6+0.1
1E 2259+586 [190]	-	P [65]	-	D [119]	-	7.5 [51]	SNR CTB 109
Soft Gamma-ray Repeaters							
SGR 0526-66 [33]	-	P [220]	-	-	-	55	LMC, SNR N49
SGR 1627-41 [261]	-	D,T [261]	-	-	-	11 [35]	
SGR 1806-20 [165]	D [186]	P [155]	-	D [153; 130]	-	15 [36]	Massive Star Cluster
SGR 1900+14 [176]	D [96]	P [123]	-	D? [233]	-	15 [248]	Massive Star Cluster

Notes:^(a) Here and throughout the whole paper I use abbreviated names. See Table 6 for the full names of these sources.^(b) D = detection; P = pulsations detected; T = transient^(c) Candidate AXP (no \dot{P} measurement)

2 Spectral Properties

2.1 X-ray Luminosity

AXPs were discovered as relatively bright (several milliCrabs²), persistent X-ray sources, and similar fluxes were later found in the X-ray counterparts of galactic SGRs. Although the lack of optical identifications hampered accurate distance estimates for the individual objects, it was clear from their collective properties (high X-ray absorption and distribution in the Galactic plane) that these objects had characteristic distances of at least a few kpc. Such values, supported in some cases by the distance estimates of the associated SNRs, implied typical luminosities in the range 10^{34-36} erg s⁻¹, clearly larger than the rotational energy loss inferred from their period and \dot{P} values³.

Durant & van Kerkwijk [51] studied the optical reddening versus distance in the fields of six AXPs in order to infer distances from the absorption measured in X-rays. This led, in a few cases, to significantly revised distance estimates (e.g. 9 ± 1.7 kpc wrt ~ 3 kpc for 1E 1048–59; 3.1 ± 0.5 kpc wrt ~ 10 kpc for XTE J1810–197). If confirmed, this result implies that the persistent luminosities of AXPs (<10 keV) are all tightly clustered around 1.3×10^{35} erg s⁻¹. This is quite interesting since in the magnetar model this luminosity is the expected saturation value above which rapid cooling of the NS interior is effective⁴ [237].

Unfortunately the method of Durant & van Kerkwijk [51] cannot be used for the SGRs, since they are too far and absorbed. Assuming that they have the same luminosity derived for the AXPs, one obtains $d \sim 10$ kpc and ~ 8 kpc, for SGR 1900+14 and SGR 1806–20 respectively, while their possible associations with star clusters (sect. 8.2) favor slightly larger distances. Also SGR 0526–66 in the Large Magellanic Cloud, with a well known distance implying a luminosity of $\sim 10^{36}$ erg s⁻¹ [162], does not fit in this picture. Thus there is some evidence that the SGRs might have a slightly higher luminosity than the persistent AXPs.

2.2 X-ray spectra

AXPs have soft spectra below 10 keV, that are generally fitted by a combination of a steep power-law (photon index $\sim 3-4$) and a blackbody with temperature $kT \sim 0.5$ keV [183]. In a few AXPs, equivalently good fits are obtained with two blackbodies (Fig. 1) or other combinations of two spectral

² 1 mCrab $\sim 2 \times 10^{-11}$ erg cm⁻² s⁻¹ in the 2-10 keV range.

³ With the reasonable assumption that these objects are neutron stars (moment of inertia $I_{NS} = 10^{45}$ g cm²); the fact that white dwarfs have much larger moments of inertia ($I_{WD} \gtrsim 10^4 I_{NS}$) led to propose models based on isolated white dwarfs, powered by rotational energy [204; 242].

⁴ Assuming the same luminosity for 1E 1547-54 (not included in the above analysis) favors its location at ~ 9 kpc, consistent with its radio dispersion measure [22], rather than the closer distance of 4 kpc suggested by its possible association with star forming regions in the Crux-Scutum spiral arm [86].

components. Physical arguments in favor of the double-blackbody spectrum were given by Halpern & Gotthelf [104].

Although all these models are just phenomenological descriptions of the data, they indicate that the soft X-ray emission is predominantly of thermal origin, but the emerging spectrum is more complex than a simple Planckian. This is not surprising, considering the presence of a strongly magnetized atmosphere and/or the effects of scattering in the magnetosphere. Several attempts to correctly take into account these complex phenomena have been done in recent years, leading to more physical spectral models that seem promising to explain some of the observed characteristics, such as the absence of cyclotron features and the hard X-ray tails [171; 68; 102; 198].

SGRs tend to have harder spectra below 10 keV than AXPs, with the exception of SGR 0526–66 which is the most “AXP-like” of the SGRs. They also suffer of a larger interstellar absorption, which makes the detection of blackbody-like components more difficult. Most spectra of SGR 1806–20 and SGR 1900+14 have been well fit with power-laws of photon index ~ 2 . However, when good quality spectra with adequate statistics are available, blackbody-like components with $kT \sim 0.5$ keV can be detected also in these sources (Fig. 2) [191; 185].

2.3 Features from cyclotron resonance scatter

In principle, a direct measurement of the neutron stars magnetic field could come from the detection of spectral features due to cyclotron resonance, provided that the particles (electrons or ions) responsible for the effect are securely identified. While electron lines would lie in the unobserved range above ~ 1 MeV for magnetic field strengths of $\sim 10^{14} - 10^{15}$ G, proton cyclotron features are expected to lie in the X-ray range.

The first calculations of the spectrum emerging from the atmospheres of magnetars in quiescence have confirmed this basic expectation [265; 116]. Model spectra exhibit a strong absorption line at the proton cyclotron resonance, $E_{c,p} \simeq 0.63z_G(B/10^{14} \text{ G}) \text{ keV}$, where z_G is the gravitational redshift, typically in the 0.70–0.85 range at the neutron star surface. However, despite extensive searches no convincingly significant lines have been detected up to now in the persistent emission of magnetars⁵. The tightest upper limits on the presence of lines in the 1–10 keV range have been derived with XMM-Newton [256; 191; 240; 185; 216] and Chandra [141] observations.

Some reasons have been proposed to explain the absence of cyclotron features, besides the obvious possibility that they lie outside the sampled energy range. Magnetars differ from ordinary radio pulsars not only for the field strength, but also because, as discussed in section 6.4, their magnetospheres are highly twisted and can support current flows [239]. The presence of charged particles (electrons and ions) produces a large resonant scattering depth at frequencies depending on the local value of the magnetic field, thus leading to the formation of a hard tail instead of a narrow line. A different

⁵ A report of a possible feature in 1RXS J1708–40 [215], has not been confirmed by better data [217].

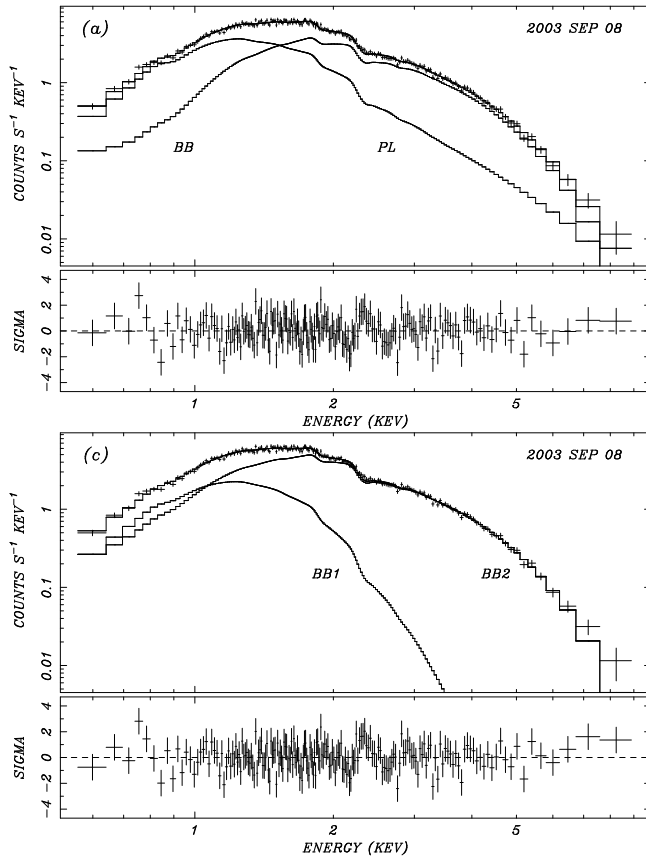


Fig. 1 X-ray spectrum of XTE J1810–197 measured with the XMM-Newton EPIC instrument (from Halpern & Gotthelf [104]). Equivalently good fits are obtained with a power law plus blackbody model (top panel) or with the sum of two blackbodies (bottom panel). The second model has the advantage that, when extrapolated to lower energies, it does not exceed the optical and near infrared limits.

explanation for the lack of lines involves vacuum polarization effects. It has been calculated that in strongly magnetized atmospheres this effect can significantly reduce the equivalent width of cyclotron lines, thus making their detection more difficult [117].

The situation is possibly different for what concerns the bursts, for which several line features have been reported in RXTE data, although not always with high statistical significance. An emission line at 6.4 keV was detected in SGR 1900+14 during the precursor burst of the 1998 August 29 intermediate flare [224]. Evidence for lines during some bursts has also been claimed for SGR 1806–20 [126; 128]. Lines were reported also from AXPs: in two bursts from 1E 1048–59 [82; 84] and in single bursts from XTE J1810–197 [258] and 4U 0142+61 [78]. For these three sources the lines were at ~ 13 –14 keV.

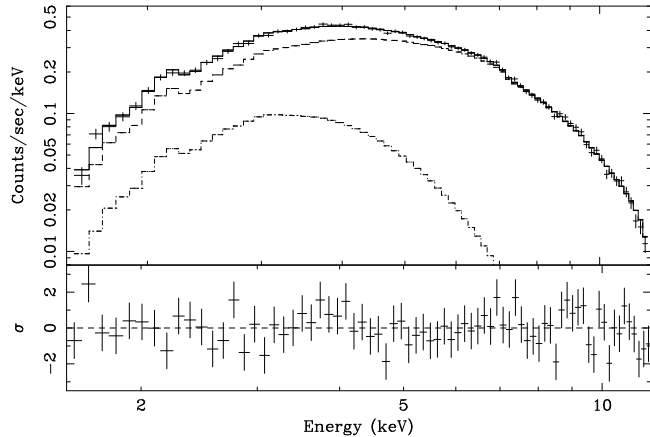


Fig. 2 XMM-Newton EPIC spectrum of SGR 1806–20 fitted with a power law plus blackbody model (from Mereghetti et al. [191]). The blackbody component is the lower curve. Notice, in comparison to Fig. 1, the much smaller relative contribution of the blackbody component to the total flux.

It has been proposed that such features are only visible in bursts, and not in the quiescent emission, because during bursts there is a higher photon flux and/or blown off baryons that provide enough optical depth [191; 217]. However, due to their sporadic appearance, and sometimes debatable statistical significance, these features require an independent confirmation, possibly with a different instrument.

2.4 Hard X-ray emission

Until a few years ago, the detection of magnetars in the hard X-ray range was limited to the bursts and flares from SGRs. The discovery with the INTEGRAL satellite of persistent hard X-ray tails extending to ~ 150 keV in AXPs came as a surprise, considering their soft spectra below 10 keV [161; 194; 42]. The hardest spectra of SGRs made them more promising targets for hard X-ray telescopes, and indeed some indication for the presence of hard tails in SGRs were already present in earlier data. For example, in 1997 BeppoSAX detected a significant emission in the 20–150 keV range, most likely originating from SGR 1900+14 [63]. However, only with the imaging capability of the INTEGRAL IBIS telescope it was possible to unambiguously confirm the presence of persistent hard X-ray emission in two SGRs [186; 96].

Emission above $\gtrsim 20$ keV has been detected for four AXPs and two SGRs (see Table 1). The upper limits on the non-detected sources are not deep enough to exclude that they have similar hard X-ray emission. In most cases pulsations have also been seen. Long term variability of the hard X-ray flux has been significantly established for SGR 1806–20 [186] and 1RXS J1708–40 [97], and cannot be excluded in the other sources.

In the case of the AXPs, the spectra above 20 keV are well fit with rather hard power laws (Fig. 4), while the spectra of SGRs are steeper (Fig. 3).

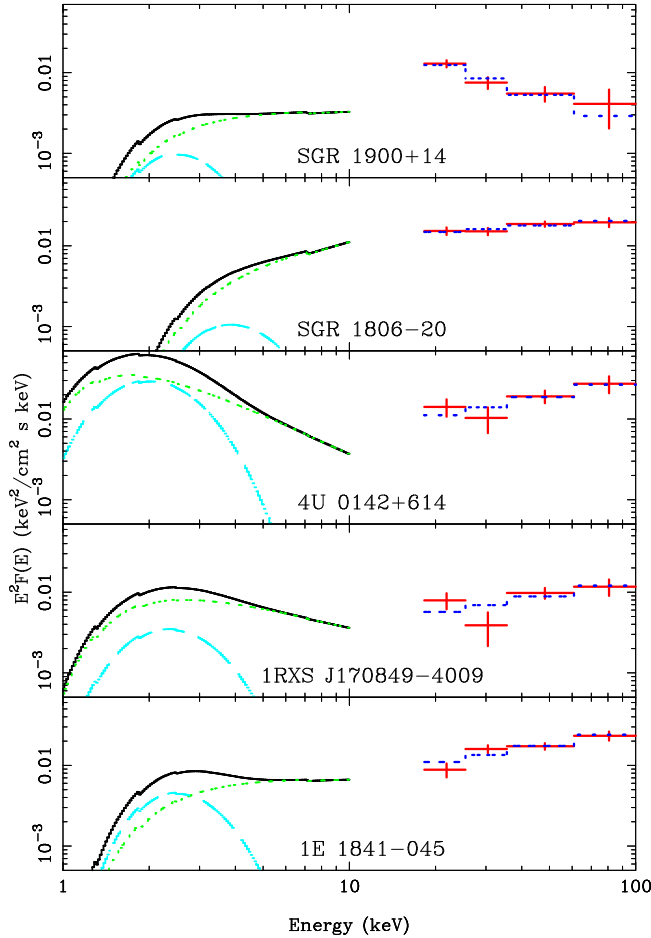
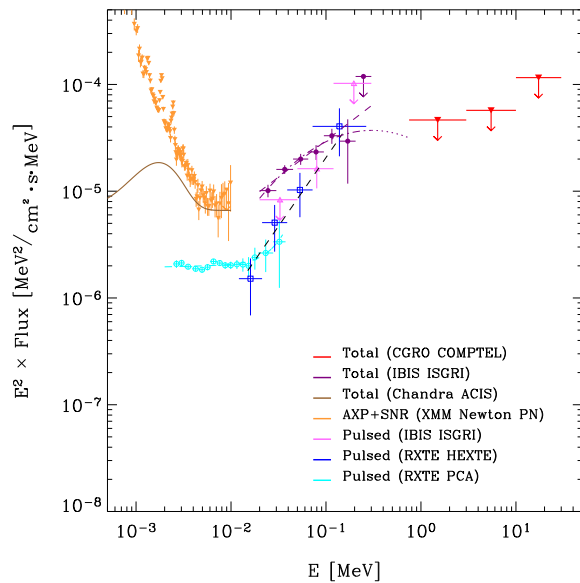
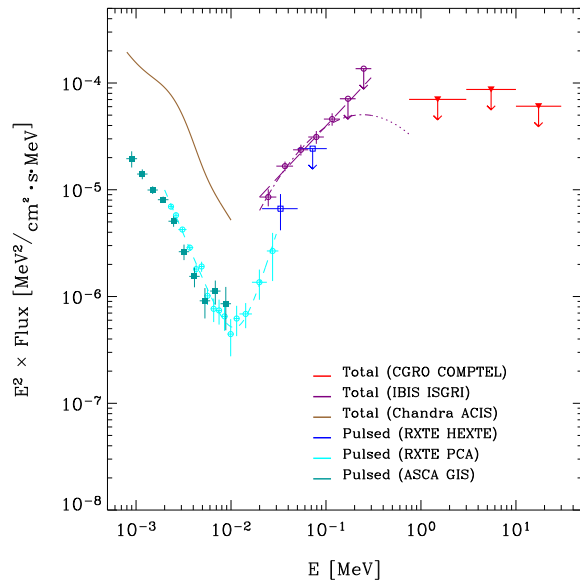
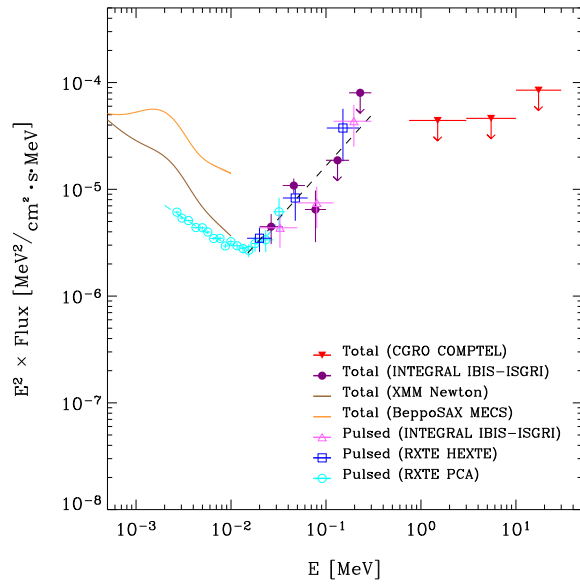


Fig. 3 XMM-Newton and INTEGRAL spectra of magnetars (from Götz et al. [96]). Note the different turn behavior of SGRs (two top panels) and AXPs: in the latter sources the spectra turn upward above 10 keV, while in the SGRs the spectra steepen.

The power law photon indexes $\Gamma \sim 1-2$ seen in the AXPs [160] imply a spectral flattening in the 10-20 keV range, and indicate that the hard X-ray tails above 10 keV and the steep power law often used in the spectral fits at lower energies are two clearly distinct components. Most importantly, the flat spectra imply that the energy released in the hard X-ray range is a significant fraction of the total energy output from these sources. The spectra obtained by considering only the pulsed flux are harder than those of the total flux, indicating that the pulsed fraction increases with energy. The most striking case is 4U 0142+61 for which the pulsed emission has a power law photon index $\Gamma = -0.8$ [160].



3 Variability Properties

3.1 Short Bursts

SGRs are characterized by periods of activity during which they emit numerous short bursts in the hard X-ray / soft gamma-ray energy range. This is indeed the defining property that led to the discovery of this class of high-energy sources. The bursts have peak luminosity up to $\sim 10^{42}$ erg s⁻¹ and durations typically in the range ~ 0.01 -1 s, with a lognormal distribution peaking at ~ 0.1 s. Most of the bursts consist of single or a few pulses with fast rise times, usually shorter than the decay times. Some examples of bursts light curves are shown in Fig. 5. The waiting time between bursts is also distributed lognormally [124] and no correlations exist between the bursts intensity and waiting time. SGR bursts occur randomly distributed in rotational phase.

The bursts observed fluences span the range from a few 10^{-10} to $\sim 10^{-5}$ erg cm⁻², and follow a power law distribution, with some evidence for a flattening at lower values [99; 95]. Since the faintest end of the distribution has been explored with instruments operating at lower energy, it is currently unclear whether the flattening reflects an energy or an intensity dependence.

Until a few years ago, SGRs bursts were mainly observed above ~ 15 keV, where their spectra could be well fitted by optically thin thermal bremsstrahlung models with $kT \sim 30$ -40 keV. More recent observations extending to lower energy (~ 1 -2 keV) showed that, if the same absorption is assumed for the burst and the persistent emission, the bremsstrahlung fits overestimate the low energy flux the bursts [67] (see Fig. 6. One solution is to invoke a higher absorption for the bursts, but there are no strong physical arguments to support this. Alternatively, good fits over the broad energy range from 1 to 100 keV can be obtained with the sum of two blackbody models with temperatures $kT_1 \sim 2$ -4 keV and $kT_2 \sim 8$ -12 keV [69; 202; 64].

The discovery with RXTE that also AXPs can emit short burst [149; 148], similar to those of the SGRs, confirmed the link between these two classes of objects and supported the application of the magnetar model also to the AXPs. Bursts have now been detected in several AXPs (see Table 3). According to Woods et al. [258] their properties suggest the existence of two distinct classes: *type A* bursts with short and symmetric profiles, and longer *type B* bursts with extended tails lasting tens to hundreds seconds. The latter have thermal spectra, tend to occur at the phases of pulse maximum, and have only been observed in AXPs⁶. Although type A bursts are the ones typically observed in SGRs, at least one AXP (1E 2259+586) showed both types of bursts. This indicates that, even if possibly originating from different mechanisms, these are not mutually exclusive. Woods et al. [258] suggested that type A bursts are caused by magnetic reconnections and type B ones by crustal fractures.

⁶ Although long decaying tails have been sometimes observed also in SGRs, they occurred only after very bright bursts and with very small ratios between the energy in the tail and that in the burst.

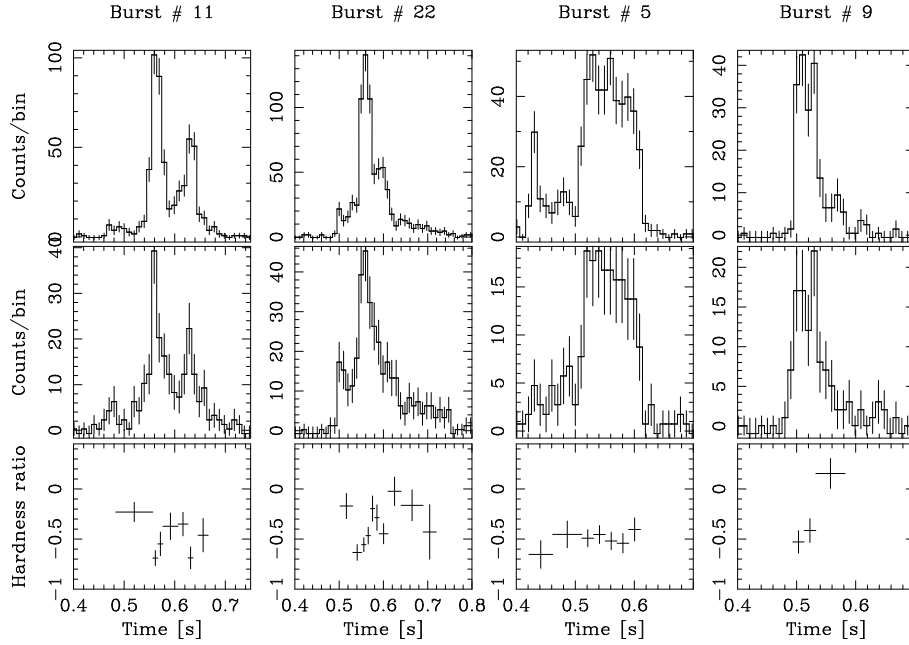


Fig. 5 Short bursts from SGR 1806–20 observed with the IBIS instrument on board INTEGRAL (from Götz et al. [94]). Top panels: light curves in the soft energy range $S=15\text{--}40$ keV. Middle panels: light curves in the hard energy range $H=40\text{--}100$ keV. Bottom panel: hardness ratios, defined as $(H-S)/(H+S)$, showing that spectral evolution is present in some burst.

3.2 Giant flares

Giant flares have been observed so far only from SGRs (see Table 2). They are characterized by the sudden release of an enormous amount of energy ($\sim(2\text{--}500)\times 10^{44}$ ergs), a fraction of which escapes directly as a relativistically expanding electron/positron plasma, while the remaining part is gradually radiated by a thermal fireball trapped in the magnetosphere. This gives to the giant flares a unique spectral and timing signature consisting of a short hard spike followed by a longer pulsating tail (Fig. 7). These two characteristic features⁷ have been clearly recognized in the giant flares observed to date, despite the differing quality and quantity of the available data.

The initial spikes of hard radiation reach a peak luminosity⁸ larger than $\sim 4 \times 10^{44}$ erg s^{-1} (up to a few 10^{47} erg s^{-1} for SGR 1806–20). They are characterized by a rise time smaller than a few milliseconds and a duration of a few tenths of second. Most detectors are saturated by the enormous photon flux from these events. It is therefore particularly difficult to reliably measure their peak fluxes and to reconstruct the true shape of their light curves. Despite these difficulties, evidence that the initial spikes have a complex,

⁷ Other features that could be observed only in some cases are a precursor and a long lasting afterglow.

⁸ Here and in the following we quote luminosities for isotropic emission.

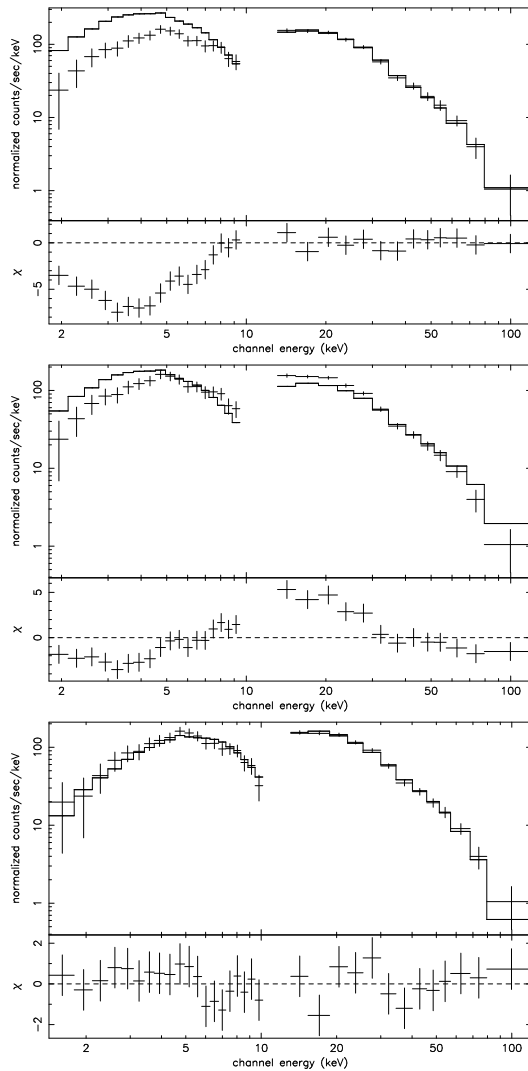


Fig. 6 Cumulative spectrum of 10 bursts from SGR 1900+14 observed with BeppoSAX (from Feroci et al. [69]). Data are from the MECS (<10 keV) and PDS (>20 keV) instruments. *Top panel:* an optically thin thermal bremsstrahlung (OTTB) model is fitted only to the PDS data; this model over predicts the flux in the MECS energy range. *Middle panel:* the OTTB model fitted to the PDS and MECS data gives unacceptable residuals. *Bottom panel:* fit to the PDS and MECS data with the sum of two blackbody models.

structured profile has been reported for the 2004 giant flare of SGR 1806–20 [232; 221].

It is well established that the spectra of the initial spikes, with characteristic temperatures of hundreds of keV, are much harder than those of the normal SGR short bursts. However, the above caveats also apply to the spectral results, with the further complication that, due to the long time intervals over which spectra are generally accumulated, it is impossible to disentangle the different time variable components. For example, for the initial spike of SGR 1806–20 a cooling blackbody spectrum, with temperature varying from 230 keV to 170 keV within ~ 0.2 s, was derived using charged particle detectors on the Wind and RHESSI spacecrafts [15]. Instead the analysis of the radiation Compton-scattered from the Moon seen with the Coronas-F satellite [73], as well as the results from small particle detectors on other satellites Palmer et al. [207], favor an exponentially cut-off power-law, although with poorly constrained parameters (photon index $\Gamma=0.73^{+0.47}_{-0.64}$ and cut-off energy $E_o = 666^{+1859}_{-368}$ keV).

The giant flares pulsating tails are characterized by a strong evolution of the flux, timing and spectral properties. Their spectra are softer than those of the initial spikes: optically thin bremsstrahlung models yield typical temperatures of a few tens of keV. The better data available for the two more recent giant flares required spectral models combining cooling thermal components and power laws, sometimes extending into the MeV region [101; 15; 73]. The decaying light curves, observed for a few minutes, are strongly modulated at the neutron star rotation period, and show complex pulse profiles which evolve with time.

The energy emitted in the pulsating tails of the three giant flares was roughly of the same order ($\sim 10^{44}$ ergs), while the energy in the initial spike of SGR 1806–20 (a few 10^{46} ergs) was at least two orders of magnitude higher than that of the other giant flares (see Table 2). Since the tail emission is thought to originate from the fraction of the energy released in the initial spike that remains trapped in the neutron star magnetosphere, forming an optically thick photon-pair plasma [236], this indicates that the magnetic field in the three sources is similar. In fact the amount of energy that can be confined in this way is determined by the magnetic field strength, which is thus inferred to be of several 10^{14} G in these three magnetars.

A unique feature was detected in the SGR 1806–20 giant flare, thanks to the large collecting area in the hard X-ray range (>80 keV) of the INTEGRAL/SPI Anti-Coincidence Shield (ACS). A hard X-ray bump, peaking about 700 s after the start of the giant flare and lasting about one hour was seen after the end of the pulsating tail (Fig. 8). Despite the lack of directional information in the ACS and the non detection of pulsations, its occurrence immediately after the giant flare strongly suggested to associate this emission with SGR 1806–20 [187]. The reality of this feature and its association with SGR 1806–20 has been subsequently confirmed by independent detections, although with smaller statistics and covering different time intervals, obtained with Konus-Wind [73] and RHESSI [15] satellites. The ACS data indicate a flux decay proportional to $\sim t^{-0.85}$, and a fluence, in counts, similar to that in the pulsating tail (1-400 s time interval). Knowledge of the

Table 2 Comparison of the three giant flares from SGRs

Source	SGR 0526–66	SGR 1900+14	SGR 1806–20
Date	March 5, 1979	August 27, 1998	December 27, 2004
Assumed distance	55 kpc	15 kpc	15 kpc
Initial Spike			
Duration (s)	~ 0.25	~ 0.35	~ 0.5
Peak luminosity (erg s^{-1})	$3.6 \cdot 10^{44}$	$> 8.3 \cdot 10^{44}$	$(2 \div 5) \cdot 10^{47}$
Fluence (erg cm^{-2})	$4.5 \cdot 10^{-4}$	$> 1.2 \cdot 10^{-2}$	$0.6 \div 2$
Isotropic Energy (erg)	$1.6 \cdot 10^{44}$	$> 1.5 \cdot 10^{44}$	$(1.6 \div 5) \cdot 10^{46}$
Pulsating tail			
Duration (s)	~ 200	~ 400	~ 380
Fluence (erg cm^{-2})	$1 \cdot 10^{-3}$	$9.4 \cdot 10^{-3}$	$5 \cdot 10^{-3}$
Isotropic Energy (erg)	$3.6 \cdot 10^{44}$	$1.2 \cdot 10^{44}$	$1.3 \cdot 10^{44}$
Spectrum	kT ~ 30 keV	kT ~ 20 keV	kT ~ 15 –30 keV
Pulse Period (s)	8.1	5.15	7.56
QPO Frequencies (Hz)	43	28, 54, 84, 155	18, 30, 92.5, 150, 625, 1480

spectral shape is required to convert the counts fluence into physical units. The ACS does not provide any spectral resolution, but only for hard spectra the ACS data can be reconciled with the small fluence seen by RHESSI in the 3–200 keV range. This is also consistent with the power law with photon index 1.6 derived from a spectral analysis of the Konus-Wind data, which however refer to a time interval after the INTEGRAL detection [73]. Both the power-law time decay and the hard power law spectrum suggest an interpretation of this long-lasting hard X-ray emission in terms of an afterglow, analog to the case of γ -ray bursts. In fact, the presence of a relativistically expanding outflow generated by the giant flare is also testified by the radio observations of this event [76; 231; 100].

A few strong outbursts, involving a smaller energy than the giant flares, but definitely brighter and much rarer than the normal short bursts, have also been seen in SGRs. They are therefore called intermediate flares. The strongest one, lasting about 40 s, was observed on April 18, 2001 from SGR 1900+14 [158; 101]. It was characterized by the presence of pulsations at the neutron star rotation period, as in the tails of giant flares, but without any initial spike (Fig. 9, bottom panel). Other intermediate flares occurred in the same source on August 29, 1998 [127], only two days after the giant flare, and on April 28, 2001 [168].

3.3 Long term X-ray variability

The apparent lack of pronounced variability, as strong as that typical of accreting X-ray pulsars, was among the distinctive properties leading to the initial recognition of AXPs. Actually, some indications for (small) long term variations were present in early observations of some AXPs, but the fact

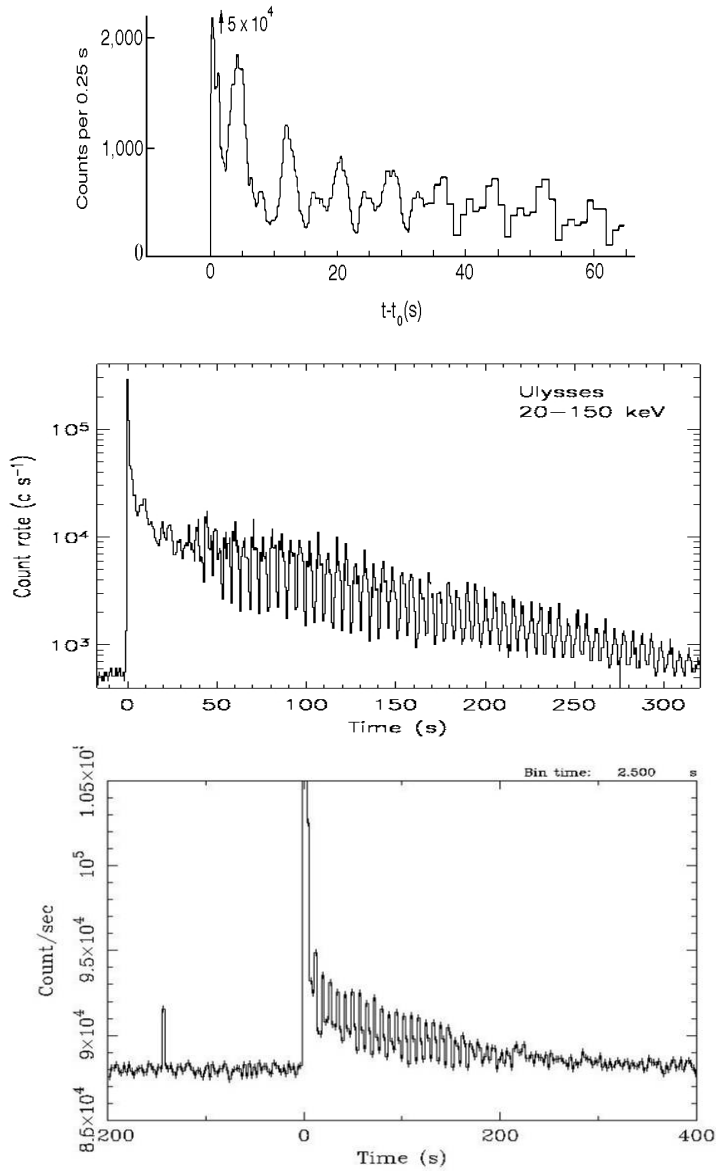


Fig. 7 Light curves of the three giant flares from SGRs. Top panel: SGR 0526-66 (Venera data in the 50-150 keV range, from Mazets et al. [175]); middle panel: SGR 1900+14 (Ulysses data in the 20-150 keV range, courtesy K. Hurley); bottom panel: SGR 1806-20 (INTEGRAL SPI/ACS at $E > 80$ keV, from Mereghetti et al. [187]). The initial peaks of the flares for SGR 0526-66 and SGR 1806-20 are out of the vertical scale.

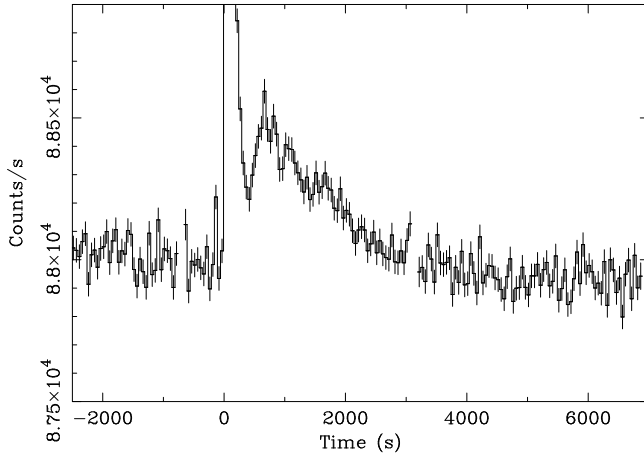


Fig. 8 SPI-ACS light curve of the SGR 1806–20 giant flare rebinned at 50 s to better show the emission lasting until one hour after the start of the outburst (from Mereghetti et al. [187]). Due to this rebinning the pulsations at 7.56 s in the time interval 0–400 s cannot be seen in this plot.

that the data were obtained with different satellites (some of which subject to source confusion due to the lack of imaging capabilities) made this evidence rather marginal. In the last decade, regular long term monitoring has been provided by the RXTE satellite, but its non-imaging instruments, unable to accurately estimate the background for faint sources, have the drawback of precisely measuring only the *pulsed* component of the flux. Changes in the pulsed flux might not reflect true luminosity variations if the pulsed fraction is not constant, as well exemplified by the case of 1E 1048–59 discussed below. In the last years, especially thanks to XMM-Newton and Chandra it has been possible to obtain much more accurate flux measurements, and practically all magnetars for which adequate data are available have shown some variability on long timescales. Besides the most extreme cases of transients, which span orders of magnitude in luminosity (section 3.4), at least two different kinds of long term variations are present in magnetars. These are well demonstrated by the cases of 1E 1048–59 and 1E 2259+586 discussed below and illustrated in Fig. 10.

For 1E 1048–59, all the measurements obtained before July 2001 had relatively large uncertainties and were consistent⁹ with an absorbed 2–10 keV flux of $\sim 5 \times 10^{-12}$ erg cm⁻² s⁻¹. Much better data were subsequently obtained with XMM-Newton and Chandra, showing unequivocal evidence for a large flux increase coupled to a decrease in the pulsed fraction [192]. The latter varied from $\sim 91\%$, when the source was at its “historical” luminosity level, to $\sim 55\%$ when the flux was more than two times higher [240]. Continued monitoring with RXTE showed that the high flux XMM-Newton and

⁹ With the possible exception of an upper limit implying a 10-fold lower flux in December 1978 [222].

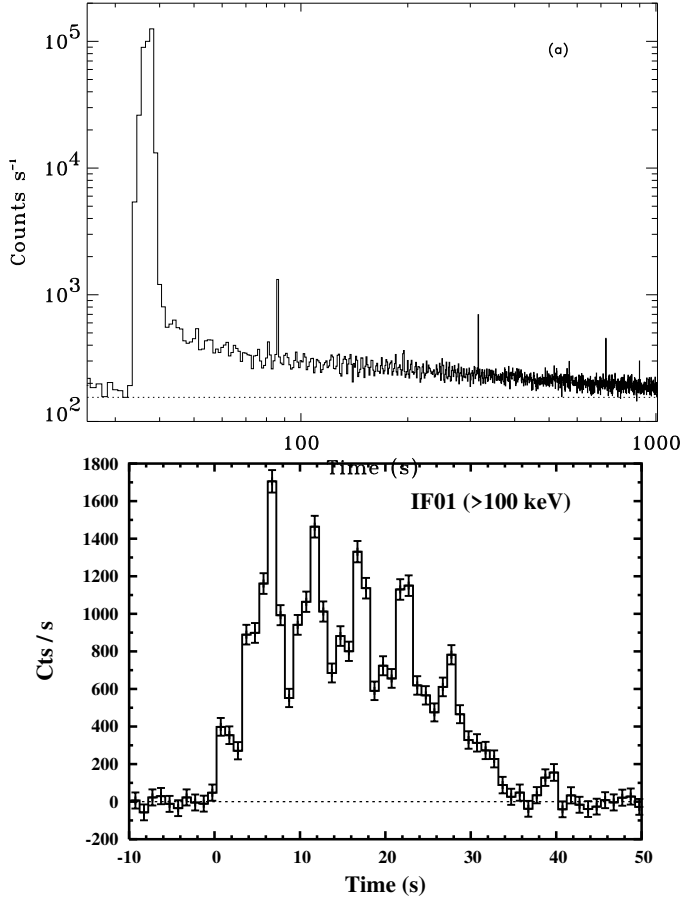


Fig. 9 Light curves of two intermediate flares from SGR 1900+14. Top panel: August 29, 1998 (RXTE, 2-90 keV, from Ibrahim et al. [127]). Bottom panel: April 18, 2001 (BeppoSAX GRBM, from Guidorzi et al. [101])

Chandra observations were obtained during long lasting outbursts¹⁰ in the *pulsed* flux intensity [81]. At the peak of the first outburst, which started in October 2001 and lasted about four months, short bursts were observed [82]. The second outburst, peaking in June 2002 was brighter and much longer.

A different behavior was seen in 1E 2259+586, when, in June 2002, RXTE observed an outburst lasting a few hours during which many tens of short bursts were emitted while the pulsed and persistent X-ray fluxes were more than one order of magnitude higher than in the usual state [148; 256]. A large glitch was also observed (see sect. 4.2). The initial rapid flux decay,

¹⁰ I shall not use the term “flare” often used to refer to these flux variations in order to avoid confusion with the SGRs flares discussed in section 3.2.

accompanied by significant evolution in the spectrum and pulse profile, was followed by a slower decline lasting months (see Fig. 11).

These two examples show that long term variations can occur either as gradual changes in the flux, often accompanied by variations in the spectrum, pulse profiles, and spin-down rate, or as sudden outbursts associated with energetic events occurring on short timescales, such as glitches and bursts¹¹. In the first case it is possible that the variations are driven by plastic deformations in the crust causing changes in the magnetic currents configurations. As discussed below (sect. 6.4), the currents supported in twisted magnetospheres are ultimately responsible for the X-ray emission through resonant cyclotron scattering and surface heating. The more violent outbursts related to glitches and bursting activity could instead be due to sudden reconfigurations of the magnetosphere, when unstable conditions are reached. This can probably occur on a large range of involved energies, with the most extreme cases being the giant flares of SGRs (sect. 3.2). The subsequent cooling of the neutron star crust, heated in these events, can give rise to the observed long term decays in the soft X-ray emission.

In March 2007, 1E 1048–59 showed an outburst [228] similar to the June 2002 event of 1E 2259+586. The 2–10 keV flux measured with Swift and Chandra soon after this event was the highest ever seen from 1E 1048–59, a factor 7 larger than the historical level. This event demonstrates that the two kinds of variability are not mutually exclusive and can occur in the same source.

3.4 Transients

Transient X-ray sources have always been of great interest since they allow to explore the theoretical models over a large luminosity range and with fixed source parameters such as distance, orientation, and, presumably, magnetic field. Some evidence for the existence of transient magnetars came first from the serendipitous observation in December 1993 of AX J1845–02, a 7 s pulsar with some characteristics of AXPs [241] located in the supernova remnant G29.6+0.1 [75]. All the subsequent observations of its error region detected only much fainter sources [245; 229] suggesting the interesting possibility of a transient, but failing to confirm the AXP nature of this source by measuring a spin-down.

The discovery of XTE J1810–197 provided a much stronger case confirming the existence of transient AXPs. Its outburst started before 2003 January 23, when the source was discovered with RXTE [125] at a flux of $\sim 6 \times 10^{-11}$ erg cm⁻² s⁻¹, a factor 100 higher than that of its quiescent counterpart recovered *a posteriori* in archival data. Since January 2003 its luminosity decreased monotonically and is now approaching the pre-outburst level (Fig. 12). During the outburst the spectral and timing properties of XTE J1810–197 were

¹¹ These short bursting episodes can easily be missed in sparse observations of magnetars; indeed some variability had already been reported in 1E 2259+586 when two GINGA observations spaced by six months showed a factor two luminosity increase coupled with a significant change in the pulse profile [140].

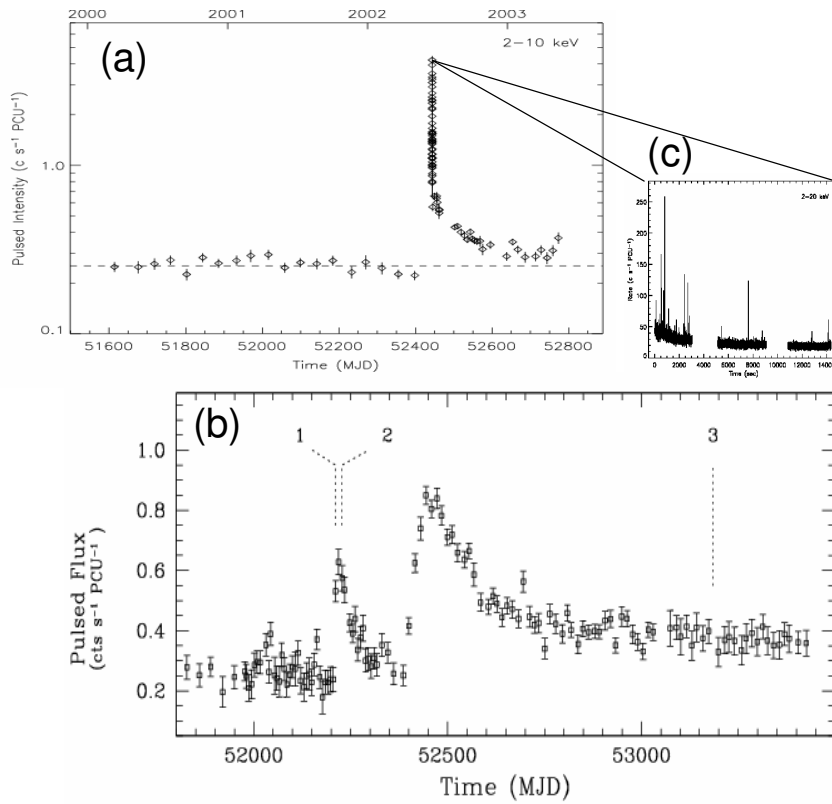


Fig. 10 Comparison of the long term variability of the two AXPs 1E 2259+586 (a) and 1E 1048-59 (b) (adapted from Gavriil et al. [83] and Woods et al. [256]). All the panels show the *pulsed* count rate as measured with RXTE in the 2-10 keV range. Note that panels (a) and (b) have approximately the same scale on the time axis, but they differ in the vertical scale that is logarithmic for 1E 2259+586. The dashed lines in panel (b) indicate the times of the three short bursts seen from 1E 1048-59. Panel (c) gives an expanded view (1 s bins) of the first four hours of the June 18, 2002 outburst from 1E 2259+586, during which many short bursts were detected

similar to those of the persistent AXPs, and short burst were also observed [258]. X-ray observations carried out during its long outburst decay showed a significant evolution of the spectrum and pulse profile [104; 89]. Gotthelf & Halpern [91] found that the spectrum is well described by two blackbody components whose luminosity decreases exponentially with different timescales. The temperature of the cooler component, initially at $kT_1 \sim 0.25$ keV, has been steadily decreasing since mid 2004, while at the same time its emitting area expanded to cover almost the whole neutron star surface. The hotter component cooled from $kT_2 \sim 0.7$ keV to $kT_2 \sim 0.45$ keV while its emitting area, initially ~ 30 km², reduced by a factor ~ 8 . This behavior has been interpreted in the framework of the magnetar coronal model [13] attributing the high temperature component to a hot spot at the footprint of an active magnetic loop and the cooler component to deep crustal heating in a large fraction of the star. As discussed below, this object is also the first magnetar from which pulsed radio emission has been detected [23].

Two other transient AXPs have been identified recently: CXOU J1647–45, in the young star cluster Westerlund 1 [195], and 1E 1547–54, likely associated to a possible SNR [86]. The first one spanned a dynamical range in luminosity larger than a factor ~ 300 . 1E 1547–54 was seen to vary only by a factor ~ 16 [107], but it is possible that the peak of the outburst was missed. Its pulsed radio emission makes it similar to the prototype AXP transient XTE J1810–197.

Only one of the four confirmed SGRs showed a transient behavior: SGR 1627–41 was discovered in 1998, when more than 100 bursts in about six weeks were observed with different satellites [261]. No other bursts have been reported since then. Its soft X-ray counterpart was identified with BeppoSAX in 1998 at a luminosity level of $\sim 10^{35}$ erg s⁻¹. Observations carried out in the following seven years showed a monotonic decrease in its luminosity, down to a level of $\sim 4 \times 10^{33}$ erg s⁻¹ (Fig. 13). The latest XMM-Newton and Chandra observations suggest that the flux stabilized at a steady level, but they are affected by relatively large uncertainties and are also compatible with a further gradual decay [184].

The behavior of SGR 1627–41 suggests a connection between the bursting activity and the luminosity of transient magnetars. The source high state coincided with a period of strong bursting activity, while in the following years, during which no bursts were emitted, its luminosity decreased. On the other hand, SGR 1806–20 and SGR 1900+14 alternated periods with and without bursts emission, but their X-ray luminosity did not vary by more than a factor two. Even more remarkably, SGR 0526–66 has a high luminosity, despite being burst-inactive since 1979. This is actually the most luminous of the SGRs, although its spectrum is rather soft and similar to those of the AXPs.

The existence of transient magnetars, with quiescent luminosities so small to prevent their discovery and/or classification, has also implications for the total number of magnetars in the Galaxy and their inferred birthrate. It is in fact likely that there is a large number of undiscovered magnetars currently in a low luminosity, quiescent state.

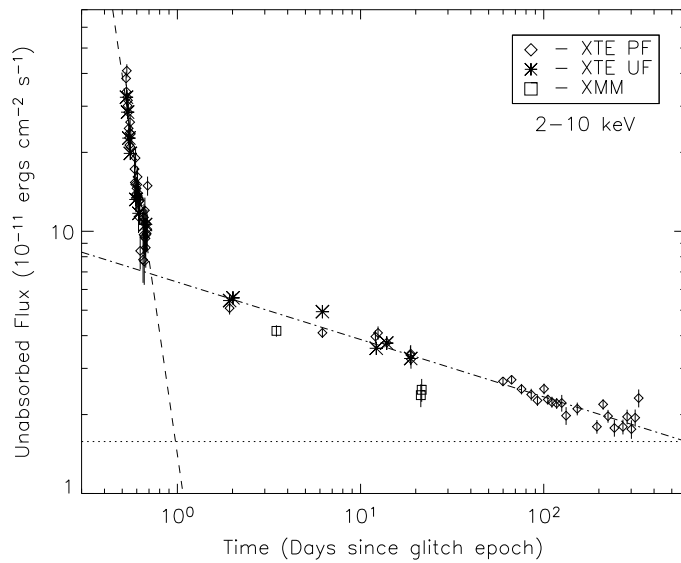


Fig. 11 Long term flux evolution of 1E 2259+586 after the June 2002 outburst (from Woods et al. [256]). During the first day the flux evolution is well fit by a steep power law with temporal index -4.5 . At later times the much slower decay is well described by a power law with index -0.2 .

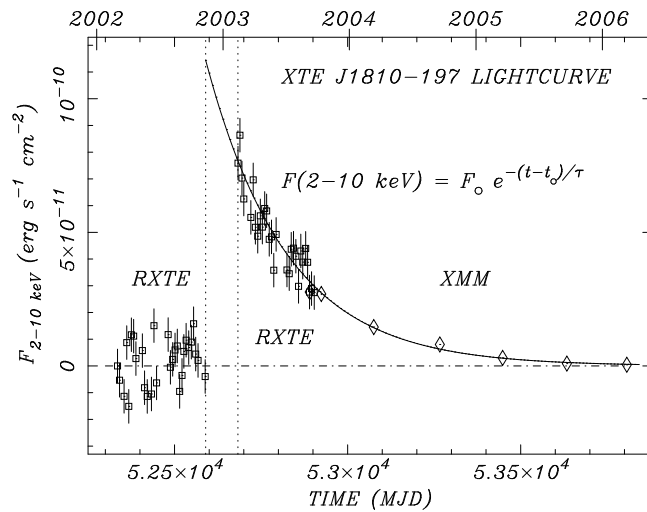


Fig. 12 X-ray light curve of the outburst of the transient AXP XTE J1810-197 (from Gotthelf & Halpern [91])

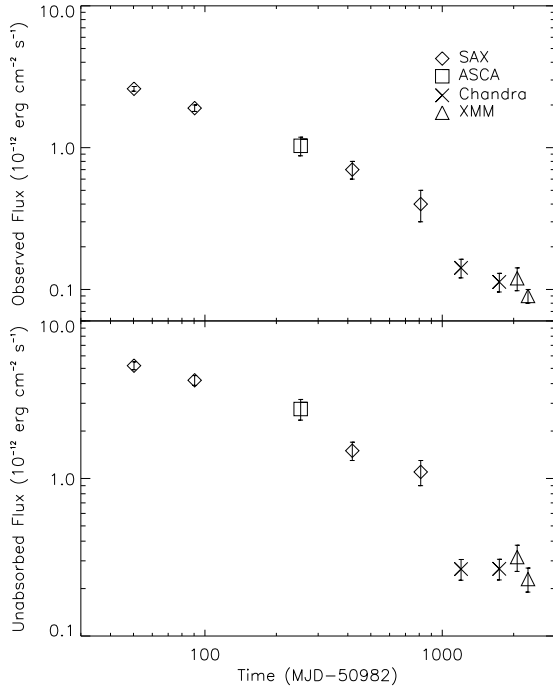


Fig. 13 Long term flux decay of SGR 1627–41 (from Mereghetti et al. [184]). Note the differences between the shape of the decays of the observed and unabsorbed fluxes (2–10 keV). The latter are subject to large uncertainties, especially at low fluxes, due to the poorly constrained spectra.

4 Timing Properties

4.1 Periods and period evolution

The narrow distribution of spin periods was among the characterizing properties that led to recognize the AXP as a separate class of objects [190]. The period range of the initial AXP group (6–12 s) has long remained unchanged with an almost tripled sample, and only recently it has been slightly extended with the discovery of an AXP, 1E 1547-54, with a spin period of 2.1 s [22]. This is still an extremely narrow distribution, compared to that of X-ray binaries (from milliseconds to hours) and radio pulsars (from 1.4 ms to 8.5 s).

While the lack of observed magnetars with periods smaller than a few seconds is easily explained by an early phase of rapid spin-down, the absence of slowly rotating objects requires some explanation [214], which, independently on the details, imply that their lifetime as bright X-ray sources is limited. In the magnetar models this could be caused, e.g. by the decay of the magnetic field [34].

The presence of periodic pulsations played an important role in the early recognition of AXPs also because it allowed to search for orbital Doppler modulations. Deep searches with RXTE failed to see any signatures of orbital motion and allowed to set stringent upper limits on the masses of potential companion stars [188; 255], showing that these objects were fundamentally different from the high mass X-ray binary pulsars.

Long term variations in the spin-down rate were already evident in some of the early AXP observations [181; 12], and were later studied in great detail thanks to phase connected timing analysis with the RXTE satellite [146; 147; 80; 259]. These observations indicate that the magnetars have a level of timing noise larger than that typically observed in radio pulsars. The timing noise is larger in the SGRs. The presence of large variations in the spin-down rate occurring on short timescales has also been confirmed by accurate timing of the radio pulses in XTE J1810–197 [20]. In addition to these gradual changes also glitches have been observed in several magnetars (section 4.2).

An overall correlation between spin-down rate and spectral hardness, with the SGRs showing the hardest spectra and larger \dot{P} , was found by Marsden & White [173]. This correlation is broadly followed also in the long term variations of the same source [191], and finds a natural explanation in the twisted magnetosphere model (sect. 6.4). However, data with a more continuous temporal coverage indicate that the situation is actually more complex, with some of the \dot{P} variations not strictly correlated to large spectral or flux changes [147; 262].

Some representative pulse profiles in the soft X-ray range are plotted in Fig. 14. Most magnetars have pulse profiles consisting of a single broad peak of nearly sinusoidal shape, while a few sources have double peaked profiles (e.g., 1E 2259+586, 4U 0142+61, CXOU J0100-72). A large variety of pulsed fractions is also observed. In most objects the pulse profiles are energy dependent and also change as a function of time. The time variations are more dramatic in the case of the SGRs [98], which tend to have more structured profiles when they are in periods of bursting activity. Strong variations in the pulse profiles have been seen to occur also on short timescales during the pulsating tails that follow the giant flares, most likely due to large scale rearrangements of the magnetic fields in the emitting regions.

In a few AXPs the pulsed fraction is smaller when the X-ray flux is higher. The best example is 1E 1048–59 [240; 228], whose pulsed fraction in the low state was $\sim 91\%$ (the highest of any magnetar) and decreased to $\sim 20\%$ when the flux increased. An anticorrelation between flux and pulsed fraction was also seen during the outbursts of June 2002 in 1E 2259+586 [256] and of September 2006 in CXOU J1647–45 [196]. The opposite behavior, i.e. a decreasing pulsed fraction, is instead seen during the long flux decay of XTE J1810–197 [91]. Finally, long term changes in the pulsed fraction of 4U 0142+61 were occurring while the overall flux remained constant [88].

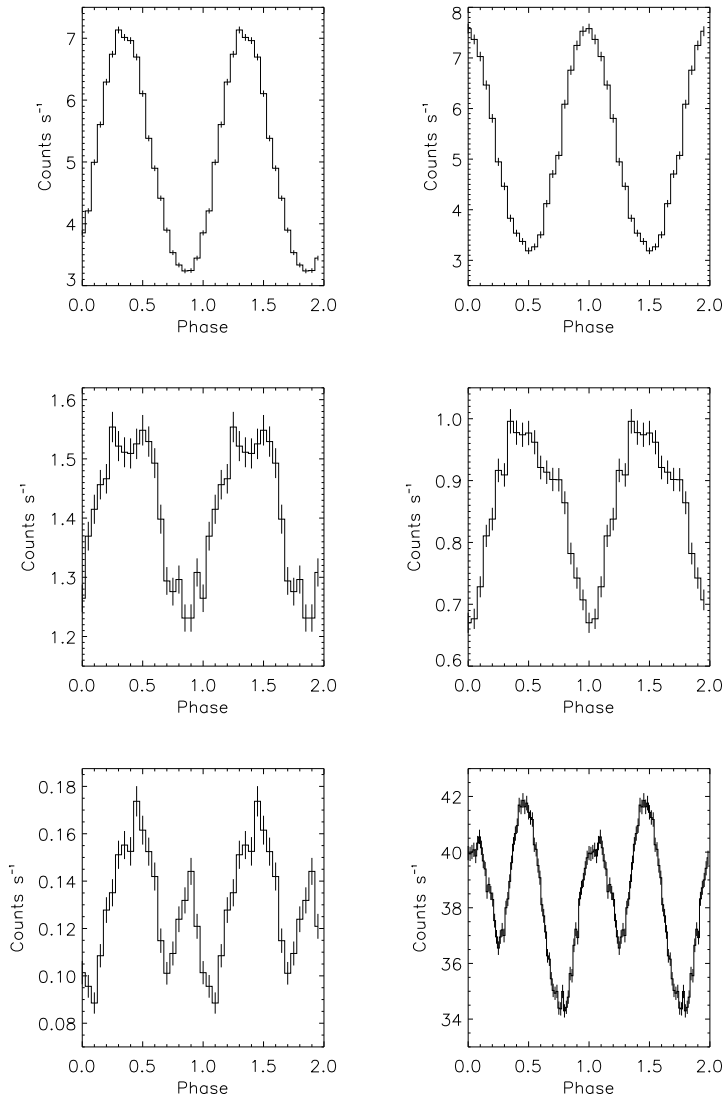


Fig. 14 Pulse profiles of AXPs and SGRs obtained with the XMM-Newton EPIC instrument in the 1-10 keV band (courtesy P.Esposito). From top left to bottom right the sources are: 1E 1048-59, XTE J1810-197, SGR 1806-20, SGR 1900+14, CXOU J0100-72 and 4U 0142+61.

4.2 Glitches

Glitches have been observed in practically all the AXPs for which adequate timing data have been taken over sufficiently long time periods (see Table 3). Most of the AXP glitch properties are consistent with those of young radio pulsars ($\tau_c \sim 10^3$ - 10^5 yr), thus giving independent evidence that AXPs and SGRs are relatively young objects. However, their glitch amplitude and frequency is larger than that seen in radio pulsars of comparable spin periods, which exhibit smaller and more rare glitches. This seems to suggest that the age of a neutron star, rather than its rotation rate, is determining the glitch properties.

The glitches in 1RXS J1708–40 have different properties in their recovery times [39], which are difficult to reconcile with a single mechanisms, such as, e.g., the standard vortex unpinning model. In particular, the recovery time after the largest glitch, was considerably shorter than typically observed in radio pulsars, and similar to that seen after the 1E 2259+586 glitch.

It seems that the variety of glitch properties in AXPs/SGRs can be better explained in terms of starquakes models. In magnetars, localized starquakes are expected due to the stresses induced by the magnetic field on the neutron star crust. The resulting movements of the magnetic foot-points are also thought to generate Alfvén waves in the magnetosphere responsible for the short burst. The June 2002 event in 1E 2259+586 [148], when both bursts and a glitch were observed, supports this scenario, while the apparent lack of bursts associated with the glitches in 1RXS J1708–40 might be due to the sparse coverage of the observations.

A large increase in the spin period was observed in connection with the August 1998 giant flare of SGR 1900+14, however the lack of adequate timing measurements in the ~ 2 months preceding this event, does not allow to distinguish among different interpretations [260]. It is possible that an “anti-glitch” (i.e. a step-like frequency *decrease*) with $\Delta P/P=10^{-4}$, coincident in time with the giant flare occurred due to a sudden unpinning of the neutron superfluid vortex lines. This requires that, contrary to ordinary neutron stars, the neutron superfluid in magnetars rotates more slowly than the crust [238]. A second possibility [206] is that the giant flare was followed by a period lasting minutes or hours with a spin-down larger by about two orders of magnitude than the long term average value of $\sim 8 \times 10^{-11}$ s s $^{-1}$. Finally, it cannot be excluded that the source underwent an increased spin-down in the two months preceding the flare. In this respect it is interesting to note that no (anti-)glitches were seen in the much more energetic giant flare of SGR 1806–20 and that the same source exhibited significant \dot{P} variations in the months preceding the giant flare [257].

Table 3 Timing parameters AXPs and SGRs

Name	P (s)	\dot{P} (s s ⁻¹)	Glitches $\Delta\nu/\nu$	Bursts
CXOU J0100-72	8.02 [164]	$1.9 \cdot 10^{-11}$ [177]		
4U 0142+61	8.69 [138]	$2 \cdot 10^{-12}$ [111; 80]	possibly one in 1998-2000? [44]	six in 2006-2007 [78]
1E 1048-59	6.45 [222]	$(1-10) \cdot 10^{-11}$ [37; 181; 81]	March 2007 [46] $(2.7 \pm 0.7) \times 10^{-6}$	two in 2001 [82] 29 June 2004 [84] with long tail
1E 1547-54	2.07 [22]	$2.32 \cdot 10^{-11}$ [22]		
CXOU J1647-45	10.6 [195]	$9.2 \cdot 10^{-13}$ [133]	21 Sept 2006 [133] 6×10^{-5}	21 Sept 2006 [133]
1RXS J1708-40	11.00 [227]	$2.4 \cdot 10^{-11}$ [135]	several [149; 39; 45; 137] $6 \times 10^{-7} - 3 \times 10^{-6}$	
XTE J1810-197	5.54 [125]	$(0.8-2.2) \cdot 10^{-11}$ [125; 89]		four from 9/2003 to 4/2004 [258]
1E 1841-045	11.77 [244]	$4.1 \cdot 10^{-11}$ [93]	three [45] $1.4 \times 10^{-6} - 5.6 \times 10^{-6}$	
AX J1845-02	6.97 [241]			
1E 2259+586	6.98 [65]	$4.8 \cdot 10^{-13}$ [80]	June 2002 [256] $(4.24 \pm 0.11) \times 10^{-6}$	>80 in June 2002 [148]
SGR 0526-66	8 [33]	$6.5 \cdot 10^{-11}$ [162]		active in 1979-1983
SGR 1627-41				active in June-July 1998
SGR 1806-20	7.6 [155]	$(0.8-8) \cdot 10^{-12}$ [155; 257]		several active periods
SGR 1900+14	5.2 [123]	$(5-14) \cdot 10^{-11}$ [157; 260]	during giant flare [260] -10^{-4}	several active periods

4.3 Quasi Periodic Oscillations

A recent interesting result is the discovery of quasi-periodic oscillations (QPO) in the decaying tails of SGRs giant flares. This phenomenon was discovered in RXTE data of the December 2004 very energetic giant flare from SGR 1806–20 [132]. QPOs at a frequency of 92.5 Hz were present in a 50 s long interval, corresponding to a bump in the unpulsed component of the X-ray emission, about 200 s after the start of the flare (see Fig. 15). They occurred only at a particular phase of the 7.6 s neutron star spin period, away from the main peak. Oscillations with a smaller significance, but lasting for a longer time interval, were also detected at lower frequencies (18 and 30 Hz).

An independent confirmation of the 92.5 Hz and 18 Hz oscillations in SGR 1806–20 was obtained with data from the RHESSI satellite, which also showed other QPOs at 26 Hz and, most remarkably, at 626.5 Hz in a different rotational phase and at higher energy [254]. Further analysis of the RXTE data of the same giant flare [226] showed other time and pulse phase dependent QPOs at ~ 150 , 625, 1480 Hz (lower significance QPOs were also present at 720 and 2384 Hz).

The discovery of QPOs in SGR 1806–20 prompted a search for the same phenomenon in the RXTE data of the August 1998 giant flare of SGR 1900+14. This led to the detection of QPOs at frequencies of 28, 54, 84 and 155 Hz [225]. The signal with the highest rms amplitude (84 Hz) was visible only for one second. The other QPOs lasted much longer (~ 90 s), and, similar to the 92.5 Hz QPO of SGR 1806–20, they were present only in a rotational phase interval, the same of the 84 Hz oscillations. In retrospect, it is also likely that the hint for a 43 Hz periodicity seen in the March 1979 flare from SGR 0526–66 [8] was due to the same phenomenon.

The QPOs observed in the tails of giant flares are most likely due to seismic oscillations induced by the large crustal fractures occurring in these extremely energetic events, similar to what happens after earthquakes. The oscillations could be limited to the crust or involve the whole neutron star, depending on the unknown amount of core-crust coupling. The correct identification of the observed vibrational modes is not obvious, with the excited harmonics probably depending on the site and nature of the crustal fracture. The theoretical models suggest that toroidal modes should be the ones most easily excited [47] and the resulting horizontal displacements could easily couple with the external magnetic field, causing the observed modulations in the X-ray flux. Given that the mode frequencies depend on the neutron star mass, radius, magnetic field, composition and structure, the QPO studies offer very interesting diagnostics, as is the case for astroseismology. In principle, it might even be possible to obtain some constraints on the neutron star equation of state.

Unfortunately, such studies are made difficult by the rarity and by the unpredictable occurrence of SGR giant flares, as well as by the fact that we do not observe directly the crust vibrations, but only their effect on the X-ray emission, mediated by the magnetic field. This is testified by the sporadic nature of the observed signals and their connection to different rotational

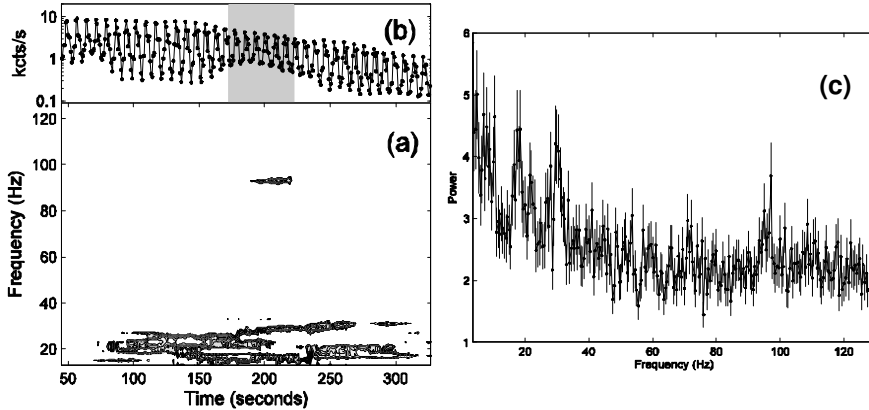


Fig. 15 QPOs in the giant flare from SGR 1806–20 (from Israel et al. [132]). The image in panel (a) shows a dynamical power spectrum, where the frequencies of the detected QPOs can be seen as a function of time. Panel (b) shows the light curve in the same time interval of panel (a). Panel (c) shows the power spectrum corresponding to the time interval 200–300 s; the peaks corresponding to QPOs at ~ 18 , ~ 30 and ~ 95 Hz are visible.

phases, probably reflecting the complex geometry of the magnetic fields and radiation beam patterns.

5 Counterparts at long wavelengths

5.1 Optical and Infrared

Much progress has been done in the search for optical/IR counterparts. Currently, counterparts have been securely identified for five magnetars and promising candidates have been detected for most of the remaining ones, thanks to the detection of objects showing variability or unusual colors inside the small error regions obtained with Chandra (and in some cases from radio observations, see Table 6).

All the (candidate) counterparts are very faint (see Table 4), giving ratios of the X-ray to IR flux larger than a few thousands. This excludes in most cases the presence of normal stars. The IR fluxes lie well below the extrap-

olation of the steep power laws often used to fit the soft X-ray spectra, but above the extrapolation of the X-ray blackbody components (Fig. 16).

After the June 2002 outburst the IR counterpart of 1E 2259+586 was a factor ~ 3 -4 brighter than the “quiescent” level [148]. The IR and X-ray fluxes subsequently decayed in a similar way, suggesting a close link between the emission processes in these two energy ranges. This was interpreted as evidence for a non-thermal, magnetospheric origin of the IR radiation [230], but Ertan et al. [62] showed that the data can also be explained as emission from a residual disk pushed away by an energetic flare and gradually relaxing back to its original configuration.

Long term IR variability has been reported also for XTE J1810–197 [218], 1RXS J1708–40 [53] (but see [233]), and SGR 1806–20 [130]. Hulleman et al. [121] found long term variability in the IR flux of 4U 0142+61, but not in the optical¹². Thus it seems that, similarly to what happened in the X-ray range, variability is detected whenever repeated accurate measurements are available. Correlations between IR and X-ray flux variations have been searched for, but a single coherent picture has not been found yet. A positive correlation was reported for flares and transient outbursts (e.g. 1E 2259+586, [148]; XTE J1810–197, [218]). In other cases the situation is more complex, and the sparse coverage of the observations does not allow to derive firm conclusions. For example, IR variations on a timescale of days have been reported for 4U 0142+61 [52], but no simultaneous X-ray data exist, and XTE J1810–197 showed fluctuations in the IR flux uncorrelated with the X-ray decay [233; 24].

These results point to possibly different origins for the X-ray and (optical)/IR emission. For example, the latter could be non thermal coherent emission from plasma instabilities above the plasma frequency [55], in which case it would be probably pulsed and polarized. Unfortunately most counterparts are too faint in the NIR to test these predictions.

4U 0142+61 is the only magnetar securely detected in the optical band, and the only one showing optical pulsations [150; 43]. The optical pulses have the same period and approximate phase of the X-rays, but a larger pulsed fraction (see also sect. 7). Possible models to explain the pulsed optical emission from 4U 0142+61 are discussed in [60].

5.2 Pulsed radio emission

Early observations to search for (pulsed) radio emission from AXPs and SGRs gave negative results¹³, although the luminosity limits were above those of many weak radio pulsars [77]. It was initially believed that the absence of radio emission was a distinctive characteristic of magnetars. This is a natural expectation in models based on accretion, that would quench any radio pulsar mechanism. For the magnetar model, it was suggested that photon splitting in

¹² However, further observations showed that also the optical flux varies [53].

¹³ Transient radio emission has been observed after the two giant flares of SGR 1900+14 [72] and SGR 1806–20 [76; 19]. This emission is thought to originate from shocks in mildly relativistic matter ejected during the giant flares [100].

Table 4 Optical and Infrared Counterparts or upper limits

Name	Counterparts	Comments and references
CXOU J0100-72		$V \gtrsim 26$ [54]
4U 0142+61	K = 19.7-20.8 R=24.9-25.6	variable, optical pulsed [120; 150; 43]
1E 1048-59	K= 19.4-21.5 $r' > 25.6$	variable [251; 250]
1E 1547-54		$K \gtrsim 17.5$ [86]
CXOU J1647-45		$K \gtrsim 21$ [253]
1RXS J1708-40		several candidates K= 18.9-19.3 [53; 233]
1E 1841-045		several candidates (K=18-21) one variable [189; 50; 233]
XTE J1810-197	K= 20.8-21.4	variable [139; 218; 233; 24]
AX J1845-02		H>21 [131]
1E 2259+586	$K_s = 21.7-20.4$ R>26.4	variable (brighter after June 2002 outburst) [119; 230]
SGR 0526-66		[144]
SGR 1627-41		$K \gtrsim 20$ [249]
SGR 1806-20	K=19.3-22	variable [130; 153]
SGR 1900+14		variable candidate K~19.7 [233; 143]

the high magnetic field could dominate over pair creation, thus suppressing the charged particle cascades that are at the origin of the radio emission [9; 10]. However, photon splitting applies only to one polarization mode: photons of the other mode cannot split. Therefore this argument does not apply, as also demonstrated by the existence of radio pulsars with inferred dipole fields of several 10^{13} G [21; 178].

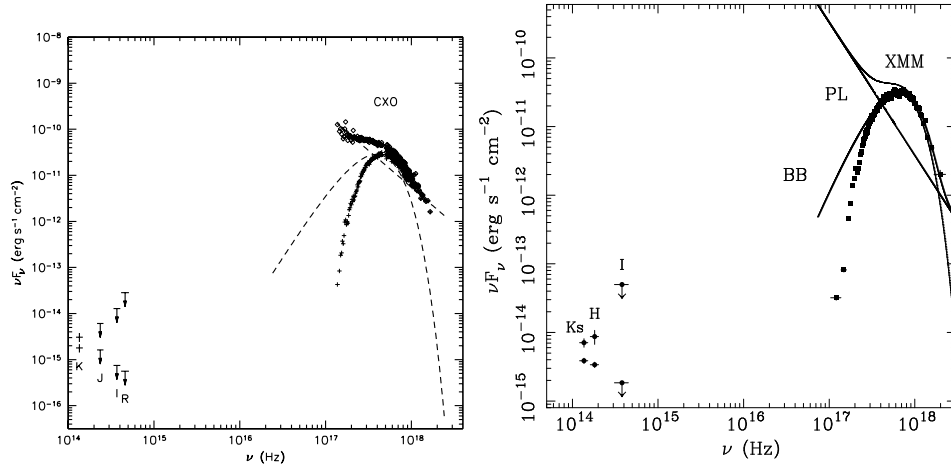


Fig. 16 Broad band spectra of 1E 2259+586 (left panel, from Hulleman et al. [119]) and XTE J1810–197 (right panel, from Israel et al. [139]). The different values for the optical/IR data refer to absorbed and unabsorbed values.

A point like radio source associated to the transient XTE J1810–197 was discovered in 2004, about one year after the start of the X–ray outburst [105], and later shown to consist of bright (>1 Jy), highly linearly polarized pulses at the neutron star rotation period [23]. The source was undetected in previous radio data, obtained before the onset of the X–ray outburst. Recently, radio pulsations at 2.07 s have been reported from 1E 1547–54 [22], thus confirming the magnetar nature of this X–ray source through a measurement of its spin-down. The fact that also this object is a transient [86] suggests that the mechanisms responsible for the pulsed radio emission in magnetars might be related to their transient nature. However, no radio pulsations were seen in the other transient AXP, CXOU J1647–45, after its September 2006 outburst [17], nor in 1E 1048–59 after the flux enhancement accompanied by a glitch that occurred in March 2007 [25]. Deep searches for radio pulsations in persistent AXPs have so far given negative results [18].

The radio properties of the two AXPs showing radio pulsations differ in several respects from those of radio pulsars: their flux is highly variable on daily timescales, their spectrum is very flat with $\alpha > -0.5$ (where $S_\nu \propto \nu^\alpha$), and their average pulse profile changes with time [27; 22; 26]. Such differences probably indicate that the radio emitting regions are more complex than the dipolar open field lines along which the radio emission in normal pulsars is thought to originate.

6 The magnetar model

6.1 Formation and evolution of magnetars

The effects of a turbulent dynamo amplification occurring either in a newly born, differentially rotating proto neutron star, or in the convective regions of its progenitor star, have been studied in detail by Thompson & Duncan [235]. They concluded that very high magnetic fields, in principle up to $3 \times 10^{17} \times (1 \text{ ms}/P_o) \text{ G}$, can be formed through an efficient dynamo if the neutron stars are born with sufficiently small periods, of the order of $P_o \sim 1\text{-}2 \text{ ms}$, and if convection is present. Population studies of radio pulsars indicate that such fast initial periods are not common, and the birth spin periods inferred from a few young pulsars are of the order of a few tens of milliseconds [66]. However, plausible mechanisms have been put forward that could lead to very high rotational speeds at least for a small fraction of the neutron star population. Rapid neutrino cooling in the proto neutron star is essential in driving the strong turbulent convection which amplifies the seed field. Such a dynamo operates only for ~ 10 seconds, but is able to generate fields as strong as 10^{16} G , most likely with a multipolar structure.

The dynamo responsible for the high magnetic field generation requires that magnetars be born with very short rotation periods. This formation scenario was predicted to have the two observational consequences discussed below: (a) magnetars could have large spatial velocities, of the order of $\sim 10^3 \text{ km s}^{-1}$ and (b) their associated supernovae should be more energetic than ordinary core collapse supernovae [49].

(a) The combination of high magnetic field and very rapid rotation is expected to impart a high velocity to the neutron star, owing to the occurrence of several possible effects, like anisotropic neutrino emission, magnetic winds, and mass ejection due, e.g., to gravitational radiation instabilities. However, up to now, the observational evidence for large spatial velocities in SGRs and AXPs is poor. The only measured proper motion has been obtained with radio VLBA observations of XTE J1810–197 [110], and corresponds to a transverse velocity of $\sim 180 \text{ (d/3 kpc) km s}^{-1}$. Most of the previously suggested associations with SNRs are now considered chance coincidences (sec. 8.1), the exceptions being the three cases where the AXP is at the remnant center and thus no high proper motion is required. The identification of possible birthplaces in massive star clusters (see section 8.2) requires spatial velocities at most of a few hundreds km s^{-1} , similar to those of radio pulsars.

(b) A large fraction of the rotational energy of a newly born magnetar, a few 10^{52} erg , is lost due to the strong magnetic braking. The initial spin-down occurs on a timescale $\sim 0.6 B_{15}^{-2} (P_o/1 \text{ ms})^2 \text{ hours}$, shorter than the supernova breakout time. Therefore, this additional injected energy should be reflected in the properties of the supernova remnant. However, an estimate of the explosion energy of the remnants containing magnetars [247] yields values close to the canonical supernova explosion energy of 10^{51} erg , implying initial periods longer than 5 ms.

The fact that these two predictions, high neutron star velocities and energetic remnants, do not seem to be fulfilled, although clearly not sufficient

to dismiss the dynamo formation mechanism, has led some support to other formation scenarios. One alternative theory is based on magnetic flux conservation arguments and postulates that the distribution of field strengths in neutron stars (and white dwarfs) simply reflects that of their progenitors. In this “fossil field” scenario, the magnetars would simply be the descendent of the massive stars with the highest magnetic fields. The wide distribution of field strengths in magnetic white dwarfs is thought to result from the spread in the magnetic fields of their progenitors. Extrapolating this result to the more massive progenitors of neutron stars could explain the origin of magnetars [70]. On average, higher magnetic fluxes are expected in the more massive progenitors. The evidence for a massive progenitor for the AXP CXOU J1647–45 in the open cluster Westerlund 1 [195], and the young clusters of massive stars found close to the locations of the SGRs (sect. 8.2), seem to support this scenario.

Another possible evidence that high magnetic fields might also be present in neutron stars born with relatively long spin periods comes from the unusual X-ray source in the supernova remnant RCW 103, if its suggested interpretation in terms of a strongly braked magnetar is confirmed (see sect. 8.4).

6.2 Origin of persistent emission and bursts

Young magnetars undergo a rapid spin down due to their strong magnetic dipole radiation losses, reaching periods of several seconds in a few thousands years. This rapid evolution toward the so called “death-line” in the B-P diagram explains why no magnetars are observed at short rotational periods, and possibly why they are not active in radio like normal pulsars (but see sect. 5.2). Shortly in their life, magnetars slow down to the point that their magnetic energy, $E_{mag} \sim 10^{47} (B/10^{15} G)^2 (R/10 \text{ km})^3 \sim 10^{46} (P/5 \text{ s}) (\dot{P}/10^{-11} \text{ s s}^{-1})$ ergs, is much larger than their rotational energy. Such a huge energy reservoir is sufficient to power for $\sim 10^4$ years the persistent X-ray emission. The giant flares sporadically emitted by SGRs, during which up to $\sim 10^{46}$ ergs can be released, are energetically more challenging. This obviously limits the number of such events that a magnetar can emit in its lifetime.

Different possibilities have been proposed to explain the observed X-ray emission at a level of several $\sim 10^{35} \text{ erg s}^{-1}$. Magnetic field decay can provide a significant source of internal heating. While ohmic dissipation and Hall drift dominate the field decay respectively in weakly ($\lesssim 10^{11} \text{ G}$) and moderately magnetized ($\sim 10^{12-13} \text{ G}$) neutron stars, the most relevant process in magnetars is ambipolar diffusion, which has a characteristic timescale $t_{amb} \sim 10^4 \times (\frac{B_{core}}{10^{15} G})^{-2}$ years [237]. This internal heating source yields a surface temperature higher than that of a cooling neutron star of the same age and smaller magnetic field. Furthermore, the enhanced thermal conductivity in the strongly magnetized envelope, contributes to increase the surface temperature [112; 115].

The motion of the magnetic field, as it diffuses out of the neutron star core, can also generate multiple small scale fractures in the crust [237]. This

persistent seismic activity produces low amplitude Alfvén waves in the magnetosphere, which can contribute to the X-ray emission, e.g., through particle acceleration leading to Comptonization and particle bombardment of the surface. Stronger and less frequent crust fractures provide a possible explanation for the short bursts.

Persistent emission in magnetars can also be induced by the twisting of the external magnetic field caused by the motions of the star interior, where the magnetic field is dominated by a toroidal component larger than the external dipole. The twisting motion of the crust sustains steady electric currents in the magnetosphere, which provide an additional source of heating for the star surface [238].

In the context of the magnetar model two mechanisms have been proposed to describe the properties of transient magnetars: deep crustal heating [170] and currents in the twisted magnetosphere [239]. The first model considers the effects that a relatively fast energy deposition in the neutron star crust, due for example to a sudden fracture or a gradual plastic deformation, has on the surface thermal emission. This model was studied primarily in connection with the “afterglows” observed after giant and intermediate flares of SGRs, but was also applied to flux decays seen on longer timescales, such as in SGR 1627–41 [156]. The time dependence of the surface “thermal echo” depends primarily on the thermal properties of the outer crust, as well as on the depth of the energy deposition. Detailed modelling of the observed light curves might thus lead to important information on the star structure. However, the available observations are far from showing a uniform picture and often subject to uncertainties that do not allow an easy comparison with the models predictions, as well exemplified [184] by the case of SGR 1627–41 shown in Fig. 13.

The radiative mechanisms responsible for the bursts and flares, which in the magnetar model are explained in terms of magnetic reconnections Lyubarsky et al. [170], are extensively discussed in Thompson & Duncan [236]. The short, soft bursts can be triggered by cracking of the crust caused by the strong magnetic field. The crust fractures perturb the magnetosphere and inject fireballs. The bursts duration is dictated by the cooling time, but it depends also on the vertical expansion of surface layers [239] and/or depth of heating [170].

A different explanation for the bursts origin has been proposed in the “fast-mode breakdown” model [113], in terms of quantum electrodynamics processes occurring in magnetic fields larger than B_{QED} . Also in this model, Alfvén waves induced by the crust motion are injected in the magnetosphere and develop discontinuities similar to hydrodynamic shocks due to the vacuum polarization. The wave energy is dissipated through electron-positron pair production and the formation of optically thick fireballs in the magnetosphere, which radiate mostly thermal emission in the hard X-ray / soft gamma-ray range.

6.3 Evidence for high magnetic fields

The secular spin-down measured in magnetars allows to infer their magnetic field through the dipole braking relation $B = 3.2 \times 10^{19} (P\dot{P})^{1/2}$ G. This yields values in the range $\sim (0.5\text{--}20) \times 10^{14}$ G. However, these estimates are subject to some uncertainties since other plausible processes, such as for example the ejection of a relativistic particles wind [108], can contribute to the torques acting on these neutron stars. Up to now, attempts to estimate the magnetic field strength through the measurement of cyclotron resonance features, as successfully done for accreting pulsars, have been inconclusive (sect. 2.3).

The most compelling evidence for the presence of high magnetic fields comes from the extreme properties of the giant flares observed in SGRs (sect. 3.2). The first object to be interpreted as a magnetar was in fact SGR 0526–66, responsible for the exceptional giant flare observed on 1979 March 5 [176]. Several properties of this event could naturally be explained by invoking a super strong magnetic field [49; 205]. The extremely challenging properties of this first observed giant flare were subsequently confirmed by the more detailed observations of similar events from two other SGRs.

Two aspects of the March 1979 event were crucial for the magnetar interpretation: its spatial coincidence with the young supernova remnant N49 in the Large Magellanic Cloud, which immediately enabled to set the energetics through a secure distance determination, and the evidence for a periodicity of 8 s, strongly hinting to the presence of a rotating neutron star. As discussed above (sect. 3.2), giant flares are characterized by an initial hard spike of emission up to the MeV range, lasting a fraction of a second, followed by a long tail (several minutes) with a softer spectrum and clearly showing the periodic modulation due to the neutron star rotation. Magnetic confinement of the hot plasma responsible for the pulsating tails is one of several evidences for the presence of a high field, and sets a lower limit of the order of a few 10^{14} G.

Other motivations for a high magnetic field include: (a) the reduction, due to the magnetic field, in the photon opacity required to exceed by at least a factor $\sim 10^3$ the Eddington limit for a neutron star in the soft γ -ray bursts; (b) the necessity of providing enough magnetic free energy to power the giant flares; (c) the short duration of the initial spikes, consistent with the propagation with Alfvén speed of the magnetic instability over the whole neutron star surface [236].

A strong dipole field also provides a natural way to slow-down a neutron star to a long period within a relatively short time. In the case of SGR 0526–66, currently spinning at 8 s, the associated SNR implies an age of $\sim 10^4$ yrs. Although most of the proposed associations of the other magnetars with SNRs are no more considered significant (sect. 8.2), their small scale height on the Galactic plane and their tendency to be found in regions of active star formation and close to clusters of very massive stars [36; 248; 152; 195] indicate that magnetars are young objects.

Finally, an independent evidence for superstrong magnetic fields in SGRs has been recently pointed out by Vietri et al. [246] who considered the high frequency QPOs observed in the giant flare of SGR 1806–20 (sect. 4.3). The

625 and 1840 Hz QPOs involve extremely large and rapid luminosity variations, with $\Delta L/\Delta t$ as large as several 10^{43} erg s $^{-2}$ (the exact value depends on the assumed beaming). This value exceeds the Cavallo-Rees luminosity-variability limit $\Delta L/\Delta t < \eta 2 \times 10^{42}$ erg s $^{-2}$, where η is the efficiency of matter to radiation conversion [28]. The relativistic effects, generally invoked to circumvent this limit (e.g. in blazars and gamma-ray bursts) are unlikely to be at work in the SGR QPO phenomenon. Vietri et al. [246] instead propose that the Cavallo-Rees limit does not apply due to the reduction in the photon scattering cross section induced by the strong magnetic field. In this way a lower limit of $\sim 2 \times 10^{15}$ G $(10 \text{ km}/R_{NS})^3 (0.1/\eta)^{1/2}$ for the surface magnetic field is derived.

6.4 Twisted magnetospheres

Thompson et al. [239] studied the properties of twisted magnetospheres threaded by large scale electrical currents. It is believed that the magnetar internal field is tightly wound up in a toroidal configuration and is up to a factor ~ 10 stronger than the external field. The unwinding of the internal field shears the neutron star crust. The rotational motions of the crust provide a source of helicity for the external magnetosphere by twisting the magnetic fields which are anchored to the star surface (see Fig. 17). A globally twisted magnetosphere, instead than a simple dipolar configuration, could be the main difference between magnetars and high B radio pulsars.

The presence of a twisted magnetosphere ($B_\phi \neq 0$) has several interesting consequences. A twisted, force-free magnetosphere supports electrical currents several orders of magnitude larger than the Goldreich-Julian current flowing along open field lines in normal pulsars. The strong flow of charged particles heats the neutron star crust and produces a significant optical depth for resonant cyclotron scattering in the magnetosphere. Repeated scattering of the thermal photons emitted at the star surface can give rise to significant high-energy tails. The optical depth is proportional to the twist angle, thus a spectral hardening is expected when the twist increases. Another consequence of the twisted field is that the spin-down torque is larger than that of a dipolar field of the same strength. Given that both the spectral hardening and the spin-down rate increase with the twist angle, a correlation between these quantities is expected. In fact the presence of such a correlation has been reported by Marsden & White [173]. Since the stresses building up in the neutron star crust lead to crustal fractures which are at the base of the burst emission, it is also expected that a twist angle increase should give rise to an enhanced bursting activity. The overall evolution of SGR 1806–20 in the years preceding the giant flare of December 2004 (see Fig. 18) seems to support these predictions [191].

The magnetar starquakes and twisting magnetic field lead to the formation of an electron/positron corona in the closed magnetosphere. The corona consists of closed flux tubes, anchored on both ends to the neutron star surface and permeated by currents driven by the twisting motion of their footpoints. The persistent hard X-ray emission extending up to ~ 100 keV originates in a transition layer between the corona and the atmosphere, while

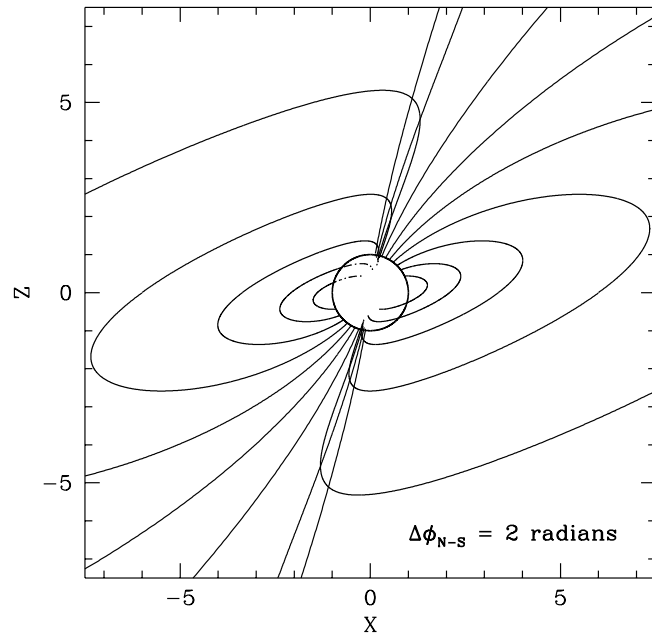


Fig. 17 Example of a twisted dipole magnetic field (from Thompson et al. [239]). The twist angle between the northern and southern hemisphere is $\Delta\phi_{N-S} = 2$ rad. Dashed lines indicate the part of the field lines behind the neutron star.

the optical and IR are emitted by curvature radiation in the corona [13]. The gradual dissipation of the magnetospheric currents can also provide plausible mechanisms for the generation of persistent soft γ -ray emission [234].

Recently, several studies concentrated on the derivation of theoretical spectral models for magnetars. Lyutikov & Gavriil [171] derived a semi-analytical model to account, in a one-dimensional approximation, for the effects of multiple resonant scatter in the magnetosphere on the blackbody emission from the magnetar surface. Their model provides a good fit to a typical AXP spectrum in the 1-10 keV range [219]. A detailed 3-D Monte Carlo simulation has been instead carried out by Fernández & Thompson [68]. Their models are quite successful to reproduce spectra and pulse profiles of AXPs in the 1-10 keV range with broad and mildly relativistic particle distributions and twist angles of ~ 0.3 -1 rad, while they over predict the thermal components of SGRs.

6.5 Hard X-ray tails

In the context of the twisted magnetosphere model, two possibilities have been proposed to explain the high-energy emission from magnetars [234]: (a) bremsstrahlung from a thin turbulent layer of the star's surface, heated to

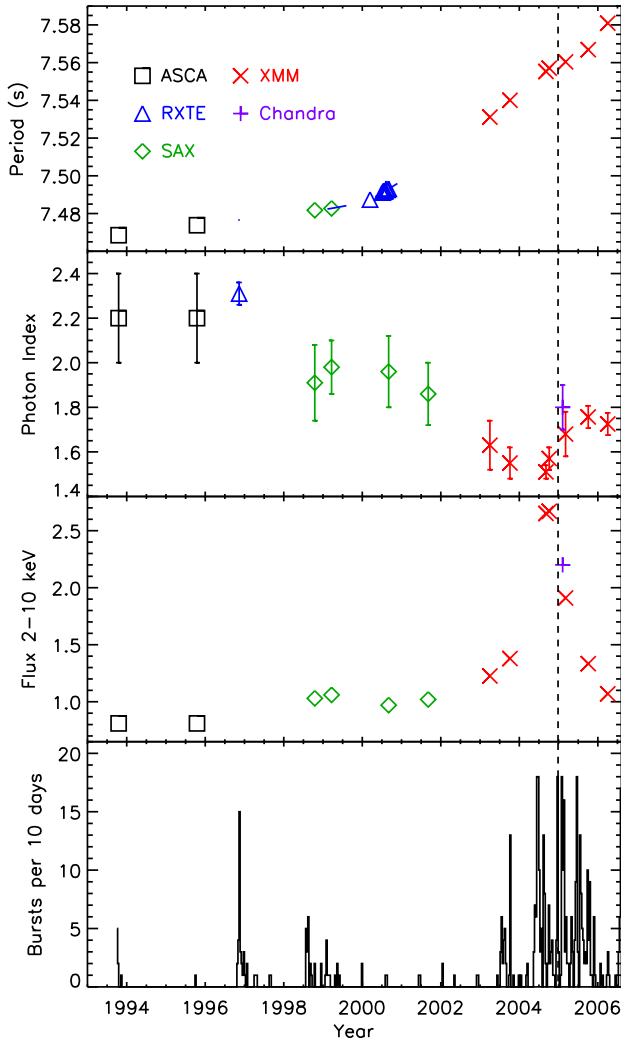


Fig. 18 Evolution of the properties of SGR 1806–20 before and immediately after the December 2004 giant flare. From top to bottom: pulse period, power-law photon index, X–ray flux, rate of bursts. The vertical line indicates the date of the giant flare. In the years preceding the giant flare the spin-down increased, the spectrum hardened, the X–ray flux and bursting activity increased (see [191] for details).

$kT \sim 100$ keV by magnetospheric currents, and (b) synchrotron emission from pairs produced at a height of ~ 100 km above the neutron star. In the first case a cut-off at a few hundred keV is expected, while in the second case the spectrum should extend to higher energies, peaking around one MeV. The currently available data are insufficient to discriminate between the two cases by measuring the energy of the spectral cut-off, which is required to avoid

exceeding the upper limits obtained with the Comptel instrument in the few MeV region.

Resonant cyclotron scattering is thought to play an important role in the production of hard X-ray emission from magnetars [11]. In strong magnetic fields the Compton scattering is resonant at the cyclotron energy, with a cross section much higher than the Thomson value. The surface thermal photons ($kT \sim keV$) propagating outward will at a given radius scatter resonantly, i.e. they are absorbed and immediately re-emitted, if there is plasma in the magnetosphere. While in normal pulsars the plasma density is too small to produce a high optical depth, this is not the case in magnetars, which have charges, with a density much higher than the Goldreich-Julian one, flowing in their magnetospheres. These charges could be accelerated along open field lines (as in radio pulsars) or they could be due to the large scale currents that are thought to be present in twisted magnetospheres. In this case they also permeate the closed field lines. Repeated scatterings of the surface thermal photons produce the hard tails. Geometry effects are important here, as well as the fact that the scattering region is large and hence the magnetic field is not homogeneous. The transmitted flux is made by the photons that on average gain energy. It is interesting to note that the scattering plasma does not need to be highly relativistic. The photon energy increase is taken at the expense of the electrons. Thus, in the case of currents in twisted magnetospheres the ultimate energy source is still the magnetic field.

According to Heyl & Hernquist [114] the hard X-ray emission could instead be due to synchrotron radiation. These authors showed that the fast-mode breakdown model they developed to explain the bursts (sect. 6.2), also predicts the presence of a non-thermal distribution of electrons and positrons in the outer parts of the magnetosphere. The quiescent hard X-ray emission, and possibly also the optical/IR, would be associated to small scale crust shifts generating fast modes whose breakdown is insufficient to produce the fireballs responsible for the bursts.

7 ALTERNATIVE MODELS

7.1 Accretion from fossil disks

Several proposals to explain the properties of the AXPs (and to a lesser extent of SGRs) are based on isolated neutron stars surrounded by residual disks. In this class of models, that in general do not require particularly high magnetic fields, the presence of a disk is invoked to account for the rapid spin-down, but different mechanisms for its formation and different origins for the observed X-ray luminosity have been considered.

It has been proposed that the AXP could be one possible outcome of the common envelope evolutionary phase of close high mass X-ray binaries, with residual accretion disk forming after the complete spiral-in of a neutron star in the envelope of its giant companion [243; 87]. For residual disks masses of about $0.01 M_{\odot}$, initial spin periods of 2-50 ms, and magnetic fields in the upper range of the distribution of normal pulsars ($\sim 10^{13}$ G), the propeller torques can spin down the neutron star to periods of a few seconds in less

than 10^4 years [31]. After the propeller phase, the neutron star can start to accrete significantly, becoming visible as an AXP with a period close to the equilibrium value, which would slowly increase owing to the decreasing accretion rate in the disk. In this model the upper cut off in the AXP period distribution is explained by invoking a significant drop in the accretion efficiency due to an advection dominated flow when the accretion rate falls below ~ 0.01 of the Eddington value [30].

Alpar [3] suggested that the properties of a fall-back disk are among the fundamental parameters, together with initial spin period and magnetic field, that determine the fate of newly born neutron stars. He proposed a scenario which attempts to unify the different classes of isolated neutron stars: radio pulsars, AXPs and SGRs, Compact Central Objects in SNRs and X-ray Dim neutron stars (see sect. 8.3 for a discussion of these objects).

According to Marsden et al. [172] the formation of disks around SGRs and AXPs is favored because, compared to normal radio pulsars, they are born in denser interstellar medium regions and have larger spatial velocities. Their supernova remnants expansion are expected to rapidly decelerate through interaction with the dense environment, thus forming strong reverse shocks that would push back part of the ejecta toward the neutron star. In addition, high velocity neutron stars might be nearly co-moving with the supernova ejecta, favoring their capture. In this model the different observational properties of AXPs and SGRs are ascribed to their birth location rather than to an intrinsic difference with the other neutron stars. However, the evidence for different birth environments claimed by Marsden et al. [172] (mostly on the basis of the relatively small dimensions of the AXPs/SGRs supernova remnants), has been criticized and disproved [48]. Furthermore, the early suggestions for association with supernova remnants for most AXPs/SGRs, on which this model is based, are no more considered significant (also implying that no large velocities are required, see sect. 8.1).

Models involving fossil disks are often criticized based on the fact that the putative disks should be visible in the optical and NIR. The expected optical/IR flux depends, among other things, on the size and orientation of the disk, as well as on the prescriptions assumed for the reprocessing of the X-ray radiation at longer wavelengths [210; 209; 120; 59]. This explains why different conclusions were drawn from such studies, as is well exemplified by the case of 4U 0142+61. This AXP is unique in showing optical pulsations [43], and has been detected over a large wavelength range, from the B band to the mid-infrared at $8 \mu\text{m}$ [252]. When its optical counterpart was identified, Hulleman et al. [120] concluded that it was too faint to be compatible with a disk, unless a particularly small disk size was invoked. The subsequent discovery of optical pulsations at the neutron star spin period [150], has been interpreted as supporting the magnetar model, on the basis that the optical (4,000-10,000 Å) pulsed fraction (27%) larger than the X-rays one ($\lesssim 10\%$) is difficult to explain in terms of reprocessing. However, this argument assumes that the X-ray pulse profile that we observe is the same of the radiation that intercepts the disk, which might not be true due to orientation and beaming effects. Recent observations of 4U 0142+61 with the Spitzer Space Telescope revealed a mid-IR counterpart at 4.5 and $8 \mu\text{m}$ [252], interpreted as

evidence for a cool ($T \sim 1000$ K) dust disk, truncated at an inner radius of $\sim 3 R_{\odot}$, and non-accreting (i.e. a "passive" disk, heated by the magnetar X-ray emission from the neutron star). On the other hand, Ertan et al. [61] showed that both the mid and near IR fluxes and the unpulsed optical emission are also consistent with an accretion disk whose inner boundary is close to the corotation radius.

A more severe criticism to accretion-based models with residual disks is that they cannot easily account for the bursts and flares. Hence some additional mechanism has to be added in order to explain these phenomena.

Finally, another possibility is that the magnetar field responsible for the bursting activity is not dipolar, but it is only present in higher order multipoles dominating near the neutron star surface. In this "hybrid" scenario [57; 58], the torque and accretion properties would be determined by the interaction between the disk and a dipolar component field, similar in strength to that of normal pulsars.

7.2 Other models

Other models, not involving neutron stars, have been put forward in alternative to the magnetar and accretion models discussed above. They are based on the possible existence of quark stars as the most stable configuration for dense compact stars [263; 118].

Solid quark stars could emit bursts and giant flares powered by gravitational energy released in star-quakes [264]. Stars made of strange quarks in the "color-flavor locked" phase are instead considered by Ouyed et al. [203]. The superconductive properties of matter in this state determine how the surface magnetic field adjusts itself to the internal field, which is confined to the vortices. During this field alignment phase, the star should be observable as a SGRs/AXPs.

P-stars made of up and down quarks in β -equilibrium with electrons in a chromo-magnetic condensate have been suggested by Cea [29]. This model still involves super strong dipolar fields, but in P-stars rather than in neutron stars.

8 RELATED OBJECTS

8.1 Supernova remnants

Three of the nine confirmed AXPs, plus the candidate AX J1845–02, are located at (or very close to) the geometrical center of shell like supernova remnants (Table 1). The associations are generally considered robust, due to the small chance probabilities of these spatial coincidences. Besides providing a way to obtain the AXPs distances, this indicates that AXPs are young objects ($\lesssim 10^4$ years) and do not have large transverse velocities. The failure to detect SNR shells around the other AXPs, despite targeted radio searches, is not in contradiction with a small age for these objects. In fact, as also

shown in the case of several radio pulsars with small characteristic ages, the remnants are not always visible, most likely owing to the different conditions of the interstellar medium in the surroundings of the supernova explosion.

Gaensler et al. [77] critically examined the proposed SNR associations for the four SGRs, which, if real, would imply large proper motions for these neutron stars. They concluded that only SGR 0526–66 might be associated with a SNR, but the probability of a chance coincidence for this SGRs lying close to the edge of N49, is not as small as for the AXPs mentioned above.

8.2 Massive star clusters

The relatively young ages of magnetars is also supported by a few possible associations with clusters of massive stars. The transient AXP CXOU J1647–45 was discovered during Chandra observations of the open cluster Westerlund 1 [195]. Clusters of massive stars were also found close to the positions of SGR 1900+14 [248], SGR 1806–20 [56; 71], and SGR 0526–66 [152] during deep observations aimed at finding their optical/IR counterparts. Although the chance probabilities of such coincidences are difficult to estimate *a posteriori*, it is plausible that at least some of these objects were born in the explosions of massive stars belonging to the clusters. The projected separations between the magnetars and the cluster centers are of ~ 0.5 –2 pc (except for SGR 0526–66, for which $d \sim 30$ pc). Considering the uncertainty in the ages, the implied transverse velocities are consistent with those of radio pulsars.

The possible association of magnetars with star clusters is of interest since it allows to set lower limits on the masses of their progenitors, that must have evolved faster than the currently observable cluster members. The young estimated ages of Westerlund 1 (4 ± 1 Myrs) and of the cluster close to SGR 1806–20 (< 4.5 Myrs) imply progenitors more massive than $40 M_{\odot}$ and $50 M_{\odot}$, respectively [195; 71], while in the case of the putative cluster of SGR 1900+14 the larger age (< 10 Myrs) gives a lower limit of only $20 M_{\odot}$.

8.3 Other classes of Isolated Neutron Stars

Observations in the X-ray, γ -ray and optical/IR bands have significantly changed the old paradigm of isolated neutron stars based mainly on the observations of the large population of radio pulsars. Different new manifestations of isolated neutron stars, besides AXPs and SGRs, have been recognized. Their existence might simply reflect a larger variety in the birth properties of neutron stars than previously thought, but it is also possible that some of these classes of neutron stars are linked by evolutionary paths.

The X-ray Dim Isolated Neutron Stars¹⁴ (XDINS) are nearby (~ 100 pc) X-ray pulsars characterized by very soft thermal spectra with blackbody temperatures in the range 40–110 eV, X-ray luminosity of 10^{30} – 10^{32} erg s⁻¹, faint optical counterparts ($V > 25$), and absence of radio emission (see [103] for a recent review). Thanks to the complete absence of non-thermal emission and, in a few cases, the measurement of parallactic distances, they are often considered ideal targets to infer the neutron star size and atmospheric composition through detailed modelling of their purely thermal emission. A possible relation with the magnetars is suggested by the fact that all the XDINS have spin periods in the 3–12 s range, and the period derivatives measured for two of them are of the order of 10^{-13} s s⁻¹. These P and \dot{P} values give characteristic ages of ~ 1 – 2 Myrs and magnetic fields of a few 10^{13} G (assuming dipole radiation braking). Magnetic fields in the $\sim 10^{13}$ – 10^{14} G range are also inferred by the broad absorption lines observed in the X-ray spectra of most XDINS, independently from their interpretation either as proton cyclotron features or atomic transition lines.

The seven objects observed within a distance of a few hundreds parsecs imply that the space density of XDINS is much higher than that of the active magnetars. XDINS could thus be the descendant of magnetars. Note that more distant XDINS cannot be observed because their very soft X-ray emission is severely absorbed in the interstellar medium.

Periods similar to those of the magnetars are also seen in the Rotating Radio Transients (RRATs) recently discovered in the Parkes Multibeam Survey [179]. These neutron stars emit short (2–30 ms) pulses of radio emission at intervals of minutes to hours. Their rotation periods, ranging from 0.4 to 7 s, could be inferred from the greatest common divisors of the time intervals between bursts. RRATs might represent a galactic population as large as that of active radio pulsars, that remained undiscovered for a long time due to lack of radio searches adequate to detect them. The pulsed X-rays detected from one of these objects have a thermal spectrum (blackbody temperature ~ 0.14 keV) and are consistent with cooling emission [180]. Period derivatives have been determined to date for three RRATs. Only one of these objects has a rather high inferred field $B = 5 \times 10^{13}$ G, while the other two have $B = 3$ and 6×10^{12} G, similar to normal radio pulsars. Thus their relation, if any, with the magnetars is unclear.

The Compact Central Objects (CCOs) form a heterogeneous group of X-ray sources unified by their location at the center of supernova remnants and by the lack of radio detections [208; 40]. These properties are shared with some of the AXPs, indicating a possible connection between magnetars and CCOs. The presence of supernova remnants implies that these are very young objects, maybe in an evolutionary stage preceding the AXP/SGR phase. However, the two CCOs for which pulsations have been determined do not support such a relation and rather indicate that these neutron stars are born with initial parameters opposite to those of magnetars. They have short

¹⁴ This name is not particularly appropriate anymore, considering that many dimmer neutron stars have been revealed after the discovery of this class of sources with the ROSAT satellite in the '90s. Only seven XDINS are known, hence the nickname of “Magnificent Seven” often used for these neutron stars.

spin periods (0.424 s and 0.105 s) and undetectable spin-down ($\dot{P} \lesssim 2.5 \cdot 10^{-16} \text{ s s}^{-1}$), yielding estimated magnetic fields smaller than a few 10^{11} G [90; 106]. The resulting characteristic ages exceed by orders of magnitude their true ages, as inferred from the associated SNRs, implying that their initial rotational periods were not too different from the current values. The low magnetic field and long initial spin periods of these objects might be causally related.

Similar P and \dot{P} have not been found in all the other CCOs, despite intensive searches, and it cannot be excluded that some of them be magnetars. Suggestions in this sense have been done, e.g., for the CCOs in RCW 103 (discussed in the next section) and in Cas A. Infrared features with apparently superluminal motion were observed outside the shell of the Cas A supernova remnant and interpreted as light echoes of a recent outburst from the CCO [159]. The geometry of two of such light echoes, at opposite sides of the remnant, is consistent with the emission from the CCO of a short pulse of radiation, beamed nearly perpendicular to the line of sight. This energetic event, that should have occurred between 1950 and 1955, would have been similar to an SGR giant flare, implying that the Cas A CCO is a magnetar. However, a recent analysis of more IR data failed to confirm this scenario and indicates that all the light echoes surrounding the remnant can be traced back to the date of the Cas A supernova explosion [151].

The most sensitive radio surveys carried out in the last decade have extended the range of observed magnetic fields¹⁵ in rotation powered pulsars, leading to the discovery of a few objects with fields approaching those of magnetars. However, no signs of magnetar-like activity, such as enhanced X-ray emission or bursts, were seen in the rotation-powered radio pulsars with the highest inferred magnetic fields (several 10^{13} G) [21; 178]. For example, PSR J1814–1744, despite having P and \dot{P} values very similar to those of the AXP 1E 2259+586 has a 2-10 keV luminosity smaller than $2 \cdot 10^{33} \text{ erg s}^{-1}$ [211]. These findings seemed to indicate that the dipole magnetic field intensity was not by itself the only element responsible for differentiating magnetars from ordinary radio pulsars. Very recently, short bursts have been discovered from the young pulsar at the center of the Kes 75 supernova remnant [79]. This object, PSR J1846–0258 ($P=0.326 \text{ s}$), is the pulsar with the smallest known characteristic age (884 yrs) and has a high field of $5 \cdot 10^{13} \text{ G}$. Its lack of radio emission was generally ascribed to beaming, but the discovery of magnetar-like activity now leads to consider also the possibility that this pulsar be truly radio silent. The bursts observed in PSR J1846–0258 are very similar to those seen in AXPs, and are accompanied by an enhancement of the persistent X-ray emission, a spectral softening and an increased timing noise [79]. The important discovery that apparently normal rotation-powered pulsars can exhibit the same kind of magnetically driven activity seen in AXPs and SGRs points to a more strict connection between radio pulsars and magnetars than previously thought.

¹⁵ as inferred from the timing parameters with the usual dipole assumption.

8.4 The CCO in RCW 103: a braked down magnetar ?

The X-ray source 1E 161348–5055 in the supernova remnant RCW 103 has unique variability properties that clearly distinguish it from the other CCOs [41]. It showed secular luminosity variations in the range 10^{33} – 10^{35} erg s⁻¹ and its flux is strongly modulated with a period of 6.7 hours (Fig. 19). No faster periods have been detected. The X-ray pulsed fraction larger than 40%, the light curve variability, and the optical/NIR limits, ruling out companion stars of spectral type earlier than M5, exclude the interpretation of the 6.7 hr modulation as the orbital period of a normal low mass X-ray binary (a possibility that is also ruled out by the young age, ~ 2 kyrs, of RCW 103). It seems thus more likely that the periodicity is due to the slow rotation of an isolated neutron star and that the observed X-ray emission is magnetically powered. In this scenario one is faced with the problem of slowing down the magnetar to such a long rotation period within the short lifetime of only a few thousand years implied by the age of the RCW 103 supernova remnant. A viable possibility [41] is that the braking was provided by the propeller effect due to the presence of a fossil disk formed from the supernova material fall-back. This evolutive path requires a neutron star initial period longer than ~ 300 ms in order to avoid the disk disruption by the relativistic outflow of the newly born active radio pulsar. If this interpretation is correct, it would support other recent evidence that high magnetic fields might also be present in NS born with long spin periods [70], contrary to the standard magnetar formation scenario discussed in section 6.1.

Alternatively, the RCW 103 CCO could be a binary formed by a very low mass star and a magnetar with a spin (quasi-)synchronous with the orbital period [212]. In this model the torque needed to slow down the neutron star can be provided by magnetic and/or material interactions, similar to the case of white dwarfs in intermediate polars.

8.5 Gamma-ray bursts

The initial short spikes characterizing SGR giant flares have spectral and duration properties similar to those of the short-hard class of gamma-ray bursts. It was therefore suggested that short gamma-ray bursts could be giant flares from SGRs in distant galaxies, for which only the bright initial peaks can be seen while the following pulsating tails remain below the detection sensitivity. Although this idea dates back to the time of the SGRs discovery (e.g. [175]), it received renewed attention after the 2004 giant flare from SGR 1806–20, due to the high peak luminosity of this event (a factor 100 larger than that of the two previously observed giant flares, if SGR 1806–20 is indeed at 15 kpc, see Table 2).

Short bursts (< 2 s) made up about one quarter of the bursts detected by BATSE, with an all-sky detection rate of ~ 170 yr⁻¹, while in other satellites, more sensitive in a lower energy range, they constitute a smaller fraction of the total GRB sample. A giant flare like that of SGR 1806–20 would have been visible by BATSE within a distance $D_{max} = \left(\frac{E_{1806}}{E_{thr}}\right)^{1/2} D_{1806}$,

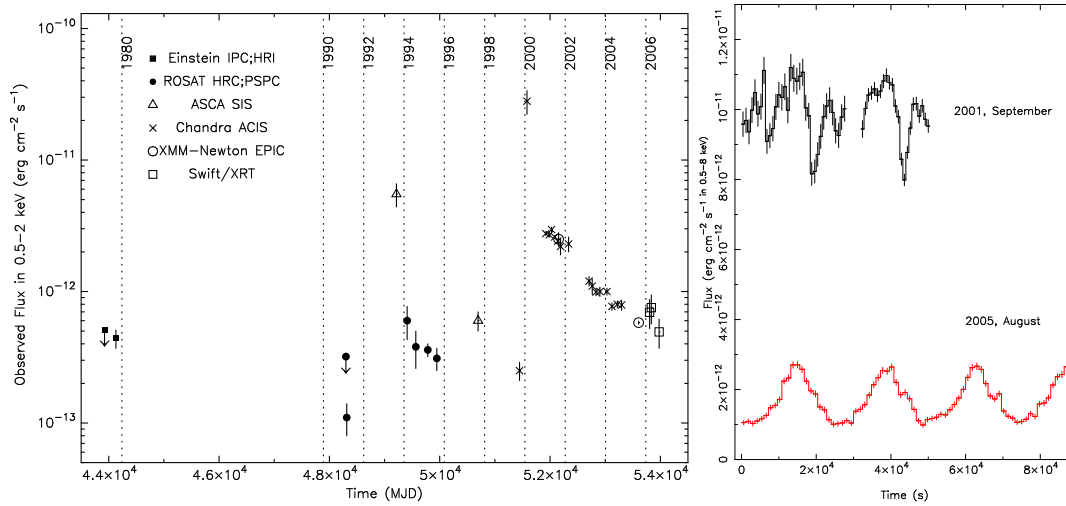


Fig. 19 Long term X-ray light curve (left panel) and pulse profiles (right panel) of the CCO in RCW 103 (from De Luca et al. [41]). Note the different pulse profiles corresponding to the two different source intensity states.

where F_{1806} is the flare peak flux (or fluence) and F_{thr} the assumed trigger threshold for BATSE. For $D_{1806}=15$ kpc, and considering the uncertainties in the above values, one obtains $D_{max} \sim 30\text{--}50$ Mpc. The expected rate of detectable SGR flares within this volume depends on further quantities not known very precisely: the frequency of giant flares in our Galaxy, estimated from only three events, and the star formation rate in the local universe compared to that in the Galaxy. In fact it is reasonable to assume that SGRs, being young objects associated with massive stars, have an abundance proportional to the star formation rate. Owing to all these factors, different estimates, ranging from $\sim 40\text{--}50\%$ [122; 207], up to 100% [197], were obtained for the fraction of short bursts in the BATSE sample that could be due to extragalactic SGRs.

However, these optimistic estimates are contradicted by several observations and analysis. No excess of short BATSE bursts is found in the direction of the Virgo cluster ($d \sim 17$ Mpc), nor short bursts were consistent with the direction of the closest galaxies with a high star formation rate [207; 213]. Searches in the error regions of a few well localized short bursts failed to detect nearby galaxies [197]. A spectral analysis of a sample of short BATSE bursts showed that only a small fraction are spectrally consistent with a SGR flare [166]. Finally, the Swift/BAT instrument, being able to detect a SGR 1806–20-like flare up to ~ 70 Mpc [122], should have observed a larger number of short bursts. All these findings suggest that some of the above assumptions are not valid. One possibility is that the distance of SGR 1806–20 be lower than 15 kpc [14]. More likely, the assumed galactic rate of one giant flare every ~ 30 years per source does not apply to the most energetic flares. Obviously these conclusions do not exclude the possibility that some of the

Table 5 Candidate extragalactic SGRs

GRB	Galaxy	distance (Mpc)	Duration (s)	Energy (ergs)	Comments	Ref.
970110	NGC 6946 ?	5.9	0.4	$2.7 \cdot 10^{44}$	possible P=13.8 s in tail	[38]
000420B	M74	10.4	0.3	$3 \cdot 10^{46}$		[199]
051103	M81	3.6	0.2	$7 \cdot 10^{46}$		[200; 74]
070201	M31	0.78	0.15	$1.5 \cdot 10^{45}$		[201; 174]

short GRBs be due to SGRs, and in fact a few candidates have been reported in recent years (see Table 5).

Gamma-ray bursts might also be associated to the formation of magnetars. Rapidly rotating, ultra-magnetized proto-neutron stars can provide the central engine required to sustain for a sufficiently long time the observed emission [16]. Metzger et al. [193] propose that the short GRBs with extended soft emission, like GRB 060614 [85] are produced by proto-magnetars formed in accretion induced collapse of white dwarfs or in the merging of white dwarf binaries. The extended emission lasting 10-100 s observed after these short bursts would result from a relativistic wind powered by the proto-magnetar rotational energy.

9 CONCLUSIONS AND FUTURE PROSPECTS

We can expect that, as usual for astronomical objects with extreme properties, the interest in AXPs and SGRs will not decrease in the coming years. In the immediate future, the prospects for large advances in the classical X-ray band are somehow limited, owing to the paucity of new missions significantly improving the capabilities of the currently available big observatories like XMM-Newton and Chandra. RXTE will soon stop operations, after a long and very successful series of observations that will be difficult to equal for what concerns all the timing aspects. XMM-Newton and Chandra have already provided a good harvest of data on most magnetars, but it is important to continue these observations especially in view of the variability phenomena discussed above. These data will remain for many year the basic reference for all the spectral models now being developed trying to include a realistic treatment of the physical processes and conditions in magnetars. Of course, new transients, as well as outbursts/flares from the known magnetars, hold the greatest potential for interesting discoveries.

The situation is more promising for what concerns the hard X-ray band, where the presence of significant emission from most magnetars has been established, but detailed studies are hampered by the relatively poor sensitivity of the current instruments. A few satellite missions (NuStar, Simbol-X, Next) are now being developed and expected to be operational after 2012. They will provide a significant step forward in sensitivity thanks to the introduction of X-ray focussing at hard X-ray energies.

On a more immediate time frame, the gamma-ray band above 100 MeV can be explored with AGILE and GLAST. In regions close to the magnetars

polar caps, the strong magnetic field is expected to quench gamma-ray emission due to pair production. However, the magnetic field is much lower in the regions considered for the gamma-ray production in outer gap models for radio pulsars. The application of such models to magnetars leads to predicted gamma-ray flux above the expected GLAST sensitivity [32]. Positive detections and phase resolved spectral studies in the MeV range would provide important comparison with rotation powered gamma-ray pulsars allowing to test the models over a wider range of the relevant parameters.

Relativistic baryons accelerated in giant flares make the SGR potential sources of neutrinos [129] and high-energy cosmic rays [6]. The AMANDA-II neutrino detector gave only an upper limit for the SGR 1806–20 December 2004 giant flare [2], and also a search for ultra high energy cosmic rays associated to this event gave a negative result [4]. However, future experiments might well confirm these prediction if other suitable giant flares are observed. Furthermore, ultra high-energy cosmic rays could be produced in the relativistic winds of rapidly spinning magnetars immediately after their birth [5].

The seismic vibrations which are thought to be at the origin of the QPOs seen in giant flares (Sect. 4.3) also produce gravitational waves. A search in the LIGO data at the frequencies seen in the SGR 1806–20 giant flare provided significant upper limits [1]. The emission of gravitational waves is also expected during the formation of magnetars. In fact, if events as powerful as the December 2004 giant flare are not unique in a magnetar lifetime, energetic arguments¹⁶ require that the internal magnetic field of a newly born magnetar be larger than 10^{16} G. Such a high field can induce a substantial deformation in the neutron star, which can give rise to the emission of gravitational waves if the rotation and symmetry axis are not aligned [223]. Thus, there is the exciting possibility that magnetars might be among the first detected sources of gravitational waves.

¹⁶ Assuming for SGR 1806–20 a distance of 15 kpc.

Table 6 Coordinates (J2000) of AXPs and SGRs

Name	X-ray position ^(a)	Uncertainty ^(c) (arcsec)	Counterparts	
CXOU J010043.1-721134	01 00 43.03 -72 11 33.6	0.5 (1σ ?) [177]		IR candidate
4U 0142+61	01 46 22.44 +61 45 03.3	0.5 (1σ ?) [141]	01 46 22.41 +61 45 03.2	opt. counterpart [120]
1E 1048-586	10 50 07.14 -59 53 21.4	0.6 (90% c.l.) [251]	10 50 07.13 -59 53 21.3	opt. counterpart [251]
1E 1547.0-5408	15 50 54.11 -54 18 23.8	0.8 (99% c.l.) [86]	15 50 54.11 -54 18 23.7	0.1 radio [22]
CXOU J164710.2-455216	16 47 10.2 -45 52 16.9	0.3 (90% c.l.) [195]		
1RXS J170849-400910	17 08 46.87 -40 08 52.44	0.7 (90% c.l.) [134]		
XTE J1810-197	18 09 51.08 -19 43 51.7	0.6 (90% c.l.) [92]	18 09 51.087 -19 43 51.93	radio [20]
1E 1841-045	18 41 19.343 -04 56 11.16	0.3 (1σ) [249]		
AX J1844.8-0256	18 44 57 -03 00	120 ^(b) (90% c.l.) [241]	18 44 54.68 -02 56 31.1	0.6 (90%) possible Chandra ctpt [229]
1E 2259+586	23 01 08.295 +58 52 44.45	0.6 (99% c.l.) [119]	23 01 08.312 +58 52 44.53	NIR ctpt [119]
SGR 0526-66	05 26 00.89 -66 04 36.3	0.6 (1σ) [162]		
SGR 1627-41	16 35 51.844 -47 35 23.31	0.2 (1σ) [249]		
SGR 1806-20	18 08 39.32 -20 24 39.5	0.3 (1σ) [142]	18 08 39.337 -20 24 39.85	NIR ctpt [130]
SGR 1900+14			19 07 14.33 +9 19 20.1	0.15 radio [72]

Notes:

(a) all the positions are from Chandra observations, except for AX J1845-02

(b) position obtained with ASCA

(c) confidence levels of the error radii are given here as reported in the corresponding references. A question mark indicates that the confidence level was not explicitly given.

References

1. Abbott, B., Abbott, R., Adhikari, R., et al. 2007, *Physical Review D*, 76, 062003
2. Achterberg, A., Ackermann, M., Adams, J., et al. 2006, *Physical Review Letters*, 97, 221101
3. Alpar, M. A. 2001, *ApJ*, 554, 1245
4. Anchordoqui, L. & for the Pierre Auger Collaboration. 2007, *ArXiv e-prints*, 706
5. Arons, J. 2003, *ApJ*, 589, 871
6. Asano, K., Yamazaki, R., & Sugiyama, N. 2006, *PASJ*, 58, L7
7. Atteia, J.-L., Boer, M., Hurley, K., et al. 1987, *ApJ*, 320, L105
8. Barat, C., Hayles, R. I., Hurley, K., et al. 1983, *A&A*, 126, 400
9. Baring, M. G. & Harding, A. K. 1998, *ApJ*, 507, L55
10. —. 2001, *ApJ*, 547, 929
11. —. 2007, *Ap&SS*, 308, 109
12. Baykal, A. & Swank, J. 1996, *ApJ*, 460, 470
13. Beloborodov, A. M. & Thompson, C. 2007, *ApJ*, 657, 967
14. Bibby, J. L., Crowther, P. A., Furness, J. P., & Clark, J. S. 2008, *ArXiv e-prints*, 802
15. Boggs, S. E., Zoglauer, A., Bellm, E., et al. 2007, *ApJ*, 661, 458
16. Bucciantini, N., Quataert, E., Arons, J., Metzger, B. D., & Thompson, T. A. 2008, *MNRAS*, 383, L25
17. Burgay, M., Rea, N., Israel, G., & Possenti, A. 2006, *The Astronomer's Telegram*, 903, 1
18. Burgay, M., Rea, N., Israel, G. L., et al. 2006, *MNRAS*, 372, 410
19. Cameron, P. B., Chandra, P., Ray, A., et al. 2005, *Nature*, 434, 1112
20. Camilo, F., Cognard, I., Ransom, S. M., et al. 2007, *ApJ*, 663, 497
21. Camilo, F., Kaspi, V. M., Lyne, A. G., et al. 2000, *ApJ*, 541, 367
22. Camilo, F., Ransom, S. M., Halpern, J. P., & Reynolds, J. 2007, *ApJ*, 666, L93
23. Camilo, F., Ransom, S. M., Halpern, J. P., et al. 2006, *Nature*, 442, 892
24. Camilo, F., Ransom, S. M., Peñalver, J., et al. 2007, *ApJ*, 669, 561
25. Camilo, F. & Reynolds, J. 2007, *The Astronomer's Telegram*, 1056, 1
26. Camilo, F., Reynolds, J., Johnston, S., Halpern, J. P., & Ransom, S. M. 2008, *ArXiv e-prints*, 802
27. Camilo, F., Reynolds, J., Johnston, S., et al. 2007, *ApJ*, 659, L37
28. Cavallo, G. & Rees, M. J. 1978, *MNRAS*, 183, 359
29. Cea, P. 2006, *A&A*, 450, 199
30. Chatterjee, P. & Hernquist, L. 2000, *ApJ*, 543, 368
31. Chatterjee, P., Hernquist, L., & Narayan, R. 2000, *ApJ*, 534, 373
32. Cheng, K. S. & Zhang, L. 2001, *ApJ*, 562, 918
33. Cline, T. L., Desai, U. D., Pizzichini, G., et al. 1980, *ApJ*, 237, L1
34. Colpi, M., Geppert, U., & Page, D. 2000, *ApJ*, 529, L29
35. Corbel, S., Chapuis, C., Dame, T. M., & Durouchoux, P. 1999, *ApJ*, 526, L29
36. Corbel, S. & Eikenberry, S. S. 2004, *A&A*, 419, 191
37. Corbet, R. H. D. & Day, C. S. R. 1990, *MNRAS*, 243, 553
38. Crider, A. 2006, in *American Institute of Physics Conference Series*, Vol. 836, *Gamma-Ray Bursts in the Swift Era*, ed. S. S. Holt, N. Gehrels, & J. A. Nousek, 64–67
39. Dall'Osso, S., Israel, G. L., Stella, L., Possenti, A., & Perozzi, E. 2003, *ApJ*, 599, 485
40. De Luca, A. 2007, *ArXiv e-prints*, 712
41. De Luca, A., Caraveo, P. A., Mereghetti, S., Tiengo, A., & Bignami, G. F. 2006, *Science*, 313, 814
42. den Hartog, P. R., Hermsen, W., Kuiper, L., et al. 2006, *A&A*, 451, 587
43. Dhillon, V. S., Marsh, T. R., Hulleman, F., et al. 2005, *MNRAS*, 363, 609
44. Dib, R., Kaspi, V. M., & Gavriil, F. P. 2007, *ApJ*, 666, 1152
45. —. 2007, *ArXiv e-prints*, 706

46. Dib, R., Kaspi, V. M., Gavriil, F. P., & Woods, P. M. 2007, *The Astronomer's Telegram*, 1041, 1
47. Duncan, R. C. 1998, *ApJ*, 498, L45+
48. —. 2002, *Memorie della Societa Astronomica Italiana*, 73, 534
49. Duncan, R. C. & Thompson, C. 1992, *ApJ*, 392, L9
50. Durant, M. 2005, *ApJ*, 632, 563
51. Durant, M. & van Kerkwijk, M. H. 2006, *ApJ*, 650, 1070
52. —. 2006, *ApJ*, 652, 576
53. —. 2006, *ApJ*, 648, 534
54. —. 2007, *ArXiv e-prints*, 711
55. Eichler, D., Gedalin, M., & Lyubarsky, Y. 2002, *ApJ*, 578, L121
56. Eikenberry, S. S., Garske, M. A., Hu, D., et al. 2001, *ApJ*, 563, L133
57. Ekşi, K. Y. & Alpar, M. A. 2003, *ApJ*, 599, 450
58. Ertan, Ü. & Alpar, M. A. 2003, *ApJ*, 593, L93
59. Ertan, Ü. & Çalıřkan, Ş. 2006, *ApJ*, 649, L87
60. Ertan, Ü. & Cheng, K. S. 2004, *ApJ*, 605, 840
61. Ertan, Ü., Erkut, M. H., Ekşi, K. Y., & Alpar, M. A. 2007, *ApJ*, 657, 441
62. Ertan, Ü., Göğüş, E., & Alpar, M. A. 2006, *ApJ*, 640, 435
63. Esposito, P., Mereghetti, S., Tiengo, A., et al. 2007, *A&A*, 461, 605
64. —. 2007, *A&A*, 476, 321
65. Fahlman, G. G. & Gregory, P. C. 1981, *Nature*, 293, 202
66. Faucher-Giguère, C.-A. & Kaspi, V. M. 2006, *ApJ*, 643, 332
67. Fenimore, E. E., Laros, J. G., & Ulmer, A. 1994, *ApJ*, 432, 742
68. Fernández, R. & Thompson, C. 2007, *ApJ*, 660, 615
69. Feroci, M., Caliendo, G. A., Massaro, E., Mereghetti, S., & Woods, P. M. 2004, *ApJ*, 612, 408
70. Ferrario, L. & Wickramasinghe, D. 2006, *MNRAS*, 367, 1323
71. Figer, D. F., Najarro, F., Geballe, T. R., Blum, R. D., & Kudritzki, R. P. 2005, *ApJ*, 622, L49
72. Frail, D. A., Kulkarni, S. R., & Bloom, J. S. 1999, *Nature*, 398, 127
73. Frederiks, D. D., Golenetskii, S. V., Palshin, V. D., et al. 2007, *Astronomy Letters*, 33, 1
74. Frederiks, D. D., Palshin, V. D., Aptekar, R. L., et al. 2007, *Astronomy Letters*, 33, 19
75. Gaensler, B. M., Gotthelf, E. V., & Vasisht, G. 1999, *ApJ*, 526, L37
76. Gaensler, B. M., Kouveliotou, C., Gelfand, J. D., et al. 2005, *Nature*, 434, 1104
77. Gaensler, B. M., Slane, P. O., Gotthelf, E. V., & Vasisht, G. 2001, *ApJ*, 559, 963
78. Gavriil, F. P., Dib, R., & Kaspi, V. M. 2007, *ArXiv e-prints*, 712
79. Gavriil, F. P., Gonzalez, M. E., Gotthelf, E. V., et al. 2008, *ArXiv e-prints*, 802
80. Gavriil, F. P. & Kaspi, V. M. 2002, *ApJ*, 567, 1067
81. —. 2004, *ApJ*, 609, L67
82. Gavriil, F. P., Kaspi, V. M., & Woods, P. M. 2002, *Nature*, 419, 142
83. —. 2004, *ApJ*, 607, 959
84. —. 2006, *ApJ*, 641, 418
85. Gehrels, N., Norris, J. P., Barthelmy, S. D., et al. 2006, *Nature*, 444, 1044
86. Gelfand, J. D. & Gaensler, B. M. 2007, *ApJ*, 667, 1111
87. Ghosh, P., Angelini, L., & White, N. E. 1997, *ApJ*, 478, 713
88. Gonzalez, M. E., Dib, R., Kaspi, V. M., et al. 2007, *ArXiv e-prints*, 708
89. Gotthelf, E. V. & Halpern, J. P. 2005, *ApJ*, 632, 1075
90. —. 2007, *ArXiv e-prints*, 704
91. —. 2007, *Ap&SS*, 58
92. Gotthelf, E. V., Halpern, J. P., Buxton, M., & Bailyn, C. 2004, *ApJ*, 605, 368
93. Gotthelf, E. V., Vasisht, G., & Dotani, T. 1999, *ApJ*, 522, L49
94. Götz, D., Mereghetti, S., Mirabel, I. F., & Hurley, K. 2004, *A&A*, 417, L45
95. Götz, D., Mereghetti, S., Molkov, S., et al. 2006, *A&A*, 445, 313

-
96. Götz, D., Mereghetti, S., Tiengo, A., & Esposito, P. 2006, *A&A*, 449, L31
 97. Götz, D., Rea, N., Israel, G. L., et al. 2007, *A&A*, 475, 317
 98. Gögüs, E., Kouveliotou, C., Woods, P. M., Finger, M. H., & van der Klis, M. 2002, *ApJ*, 577, 929
 99. Gögüs, E., Woods, P. M., Kouveliotou, C., et al. 2000, *ApJ*, 532, L121
 100. Granot, J., Ramirez-Ruiz, E., Taylor, G. B., et al. 2006, *ApJ*, 638, 391
 101. Guidorzi, C., Frontera, F., Montanari, E., et al. 2004, *A&A*, 416, 297
 102. Güver, T., Özel, F., Gögüs, E., & Kouveliotou, C. 2007, *ApJ*, 667, L73
 103. Haberl, F. 2007, *Ap&SS*, 73
 104. Halpern, J. P. & Gotthelf, E. V. 2005, *ApJ*, 618, 874
 105. Halpern, J. P., Gotthelf, E. V., Becker, R. H., Helfand, D. J., & White, R. L. 2005, *ApJ*, 632, L29
 106. Halpern, J. P., Gotthelf, E. V., Camilo, F., & Seward, F. D. 2007, *ArXiv e-prints*, 705
 107. Halpern, J. P., Gotthelf, E. V., Reynolds, J., Ransom, S. M., & Camilo, F. 2007, *ArXiv e-prints*, 711
 108. Harding, A. K., Contopoulos, I., & Kazanas, D. 1999, *ApJ*, 525, L125
 109. Harding, A. K. & Lai, D. 2006, *Reports of Progress in Physics*, 69, 2631
 110. Helfand, D. J., Chatterjee, S., Briskin, W. F., et al. 2007, *ApJ*, 662, 1198
 111. Hellier, C. 1994, *MNRAS*, 271, L21
 112. Heyl, J. S. & Hernquist, L. 1997, *ApJ*, 489, L67+
 113. —. 2005, *ApJ*, 618, 463
 114. —. 2005, *MNRAS*, 362, 777
 115. Heyl, J. S. & Kulkarni, S. R. 1998, *ApJ*, 506, L61
 116. Ho, W. C. G. & Lai, D. 2001, *MNRAS*, 327, 1081
 117. —. 2003, *MNRAS*, 338, 233
 118. Horvath, J. E. 2007, *Ap&SS*, 308, 431
 119. Hulleman, F., Tennant, A. F., van Kerkwijk, M. H., et al. 2001, *ApJ*, 563, L49
 120. Hulleman, F., van Kerkwijk, M. H., & Kulkarni, S. R. 2000, *Nature*, 408, 689
 121. —. 2004, *A&A*, 416, 1037
 122. Hurley, K., Boggs, S. E., Smith, D. M., et al. 2005, *Nature*, 434, 1098
 123. Hurley, K., Li, P., Kouveliotou, C., et al. 1999, *ApJ*, 510, L111
 124. Hurley, K. J., McBreen, B., Rabbette, M., & Steel, S. 1994, *A&A*, 288, L49
 125. Ibrahim, A. I., Markwardt, C. B., Swank, J. H., et al. 2004, *ApJ*, 609, L21
 126. Ibrahim, A. I., Safi-Harb, S., Swank, J. H., et al. 2002, *ApJ*, 574, L51
 127. Ibrahim, A. I., Strohmayer, T. E., Woods, P. M., et al. 2001, *ApJ*, 558, 237
 128. Ibrahim, A. I., Swank, J. H., & Parke, W. 2003, *ApJ*, 584, L17
 129. Ioka, K., Razzaque, S., Kobayashi, S., & Mészáros, P. 2005, *ApJ*, 633, 1013
 130. Israel, G., Covino, S., Mignani, R., et al. 2005, *A&A*, 438, L1
 131. Israel, G., Stella, L., Covino, S., et al. 2004, in *IAU Symposium*, Vol. 218, *Young Neutron Stars and Their Environments*, ed. F. Camilo & B. M. Gaensler, 247–+
 132. Israel, G. L., Belloni, T., Stella, L., et al. 2005, *ApJ*, 628, L53
 133. Israel, G. L., Campana, S., Dall’Osso, S., et al. 2007, *ApJ*, 664, 448
 134. Israel, G. L., Covino, S., Perna, R., et al. 2003, *ApJ*, 589, L93
 135. Israel, G. L., Covino, S., Stella, L., et al. 1999, *ApJ*, 518, L107
 136. —. 2002, *ApJ*, 580, L143
 137. Israel, G. L., Gotz, D., Zane, S., et al. 2007, *ArXiv e-prints*, 707
 138. Israel, G. L., Mereghetti, S., & Stella, L. 1994, *ApJ*, 433, L25
 139. Israel, G. L., Rea, N., Mangano, V., et al. 2004, *ApJ*, 603, L97
 140. Iwasawa, K., Koyama, K., & Halpern, J. P. 1992, *PASJ*, 44, 9
 141. Juett, A. M., Marshall, H. L., Chakrabarty, D., & Schulz, N. S. 2002, *ApJ*, 568, L31
 142. Kaplan, D. L., Fox, D. W., Kulkarni, S. R., et al. 2002, *ApJ*, 564, 935
 143. Kaplan, D. L., Kulkarni, S. R., Frail, D. A., & van Kerkwijk, M. H. 2002, *ApJ*, 566, 378
 144. Kaplan, D. L., Kulkarni, S. R., van Kerkwijk, M. H., et al. 2001, *ApJ*, 556, 399

145. Kaspi, V. M. 2007, *Ap&SS*, 308, 1
146. Kaspi, V. M., Chakrabarty, D., & Steinberger, J. 1999, *ApJ*, 525, L33
147. Kaspi, V. M., Gavriil, F. P., Chakrabarty, D., Lackey, J. R., & Munro, M. P. 2001, *ApJ*, 558, 253
148. Kaspi, V. M., Gavriil, F. P., Woods, P. M., et al. 2003, *ApJ*, 588, L93
149. Kaspi, V. M., Lackey, J. R., & Chakrabarty, D. 2000, *ApJ*, 537, L31
150. Kern, B. & Martin, C. 2002, *Nature*, 417, 527
151. Kim, Y., Rieke, G. H., Krause, O., et al. 2008, *ArXiv e-prints*, 801
152. Klose, S., Henden, A. A., Geppert, U., et al. 2004, *ApJ*, 609, L13
153. Kosugi, G., Ogasawara, R., & Terada, H. 2005, *ApJ*, 623, L125
154. Kothes, R. & Dougherty, S. M. 2007, *A&A*, 468, 993
155. Kouveliotou, C., Dieters, S., Strohmayer, T., et al. 1998, *Nature*, 393, 235
156. Kouveliotou, C., Eichler, D., Woods, P. M., et al. 2003, *ApJ*, 596, L79
157. Kouveliotou, C., Strohmayer, T., Hurley, K., et al. 1999, *ApJ*, 510, L115
158. Kouveliotou, C., Tennant, A., Woods, P. M., et al. 2001, *ApJ*, 558, L47
159. Krause, O., Rieke, G. H., Birkmann, S. M., et al. 2005, *Science*, 308, 1604
160. Kuiper, L., Hermsen, W., den Hartog, P. R., & Collmar, W. 2006, *ApJ*, 645, 556
161. Kuiper, L., Hermsen, W., & Mendez, M. 2004, *ApJ*, 613, 1173
162. Kulkarni, S. R., Kaplan, D. L., Marshall, H. L., et al. 2003, *ApJ*, 585, 948
163. Lamb, R. C., Fox, D. W., Macomb, D. J., & Prince, T. A. 2002, *ApJ*, 574, L29
164. —. 2003, *ApJ*, 599, L115
165. Laros, J. G., Fenimore, E. E., Fikani, M. M., Klebesadel, R. W., & Barat, C. 1986, *Nature*, 322, 152
166. Lazzati, D., Ghirlanda, G., & Ghisellini, G. 2005, *MNRAS*, 362, L8
167. Leahy, D. A. & Tian, W. 2007, *ArXiv e-prints*, 709
168. Lenters, G. T., Woods, P. M., Goupell, J. E., et al. 2003, *ApJ*, 587, 761
169. Leyder, J.-C., Walter, R., & Rauw, G. 2008, *A&A*, 477, L29
170. Lyubarsky, Y., Eichler, D., & Thompson, C. 2002, *ApJ*, 580, L69
171. Lyutikov, M. & Gavriil, F. P. 2006, *MNRAS*, 368, 690
172. Marsden, D., Lingenfelter, R. E., Rothschild, R. E., & Higdon, J. C. 2001, *ApJ*, 550, 397
173. Marsden, D. & White, N. E. 2001, *ApJ*, 551, L155
174. Mazets, E. P., Aptekar, R. L., Cline, T. L., et al. 2007, *ArXiv e-prints*, 712
175. Mazets, E. P., Golenetskii, S. V., Gurian, I. A., & Ilinskii, V. N. 1982, *Ap&SS*, 84, 173
176. Mazets, E. P., Golentkii, S. V., Ilinskii, V. N., Aptekar, R. L., & Guryan, I. A. 1979, *Nature*, 282, 587
177. McGarry, M. B., Gaensler, B. M., Ransom, S. M., Kaspi, V. M., & Veljkovic, S. 2005, *ApJ*, 627, L137
178. McLaughlin, M. A., Lorimer, D. R., Lyne, A. G., et al. 2004, in *IAU Symposium*, Vol. 218, *Young Neutron Stars and Their Environments*, ed. F. Camilo & B. M. Gaensler, 255–+
179. McLaughlin, M. A., Lyne, A. G., Lorimer, D. R., et al. 2006, *Nature*, 439, 817
180. McLaughlin, M. A., Rea, N., Gaensler, B. M., et al. 2007, *ApJ*, 670, 1307
181. Mereghetti, S. 1995, *ApJ*, 455, 598
182. Mereghetti, S., Chiarlone, L., Israel, G. L., & Stella, L. 2002, in *Neutron Stars, Pulsars, and Supernova Remnants*, ed. W. Becker, H. Lesch, & J. Trümper, 29–+
183. Mereghetti, S., De Luca, A., Caraveo, P. A., et al. 2002, *ApJ*, 581, 1280
184. Mereghetti, S., Esposito, P., Tiengo, A., et al. 2006, *A&A*, 450, 759
185. —. 2006, *ApJ*, 653, 1423
186. Mereghetti, S., Götz, D., Mirabel, I. F., & Hurley, K. 2005, *A&A*, 433, L9
187. Mereghetti, S., Götz, D., von Kienlin, A., et al. 2005, *ApJ*, 624, L105
188. Mereghetti, S., Israel, G. L., & Stella, L. 1998, *MNRAS*, 296, 689
189. Mereghetti, S., Mignani, R. P., Covino, S., et al. 2001, *MNRAS*, 321, 143
190. Mereghetti, S. & Stella, L. 1995, *ApJ*, 442, L17
191. Mereghetti, S., Tiengo, A., Esposito, P., et al. 2005, *ApJ*, 628, 938

-
192. Mereghetti, S., Tiengo, A., Stella, L., et al. 2004, *ApJ*, 608, 427
 193. Metzger, B. D., Quataert, E., & Thompson, T. A. 2007, *ArXiv e-prints*, 712
 194. Molkov, S. V., Cherepashchuk, A. M., Lutovinov, A. A., et al. 2004, *Astronomy Letters*, 30, 534
 195. Muno, M. P., Clark, J. S., Crowther, P. A., et al. 2006, *ApJ*, 636, L41
 196. Muno, M. P., Gaensler, B. M., Clark, J. S., et al. 2007, *MNRAS*, 378, L44
 197. Nakar, E., Gal-Yam, A., Piran, T., & Fox, D. B. 2006, *ApJ*, 640, 849
 198. Nobili, L., Turolla, R., & Zane, S. 2008, *ArXiv e-prints*, 802
 199. Ofek, E. O. 2007, *ApJ*, 659, 339
 200. Ofek, E. O., Kulkarni, S. R., Nakar, E., et al. 2006, *ApJ*, 652, 507
 201. Ofek, E. O., Muno, M., Quimby, R., et al. 2007, *ArXiv e-prints*, 712
 202. Olive, J.-F., Hurley, K., Sakamoto, T., et al. 2004, *ApJ*, 616, 1148
 203. Ouyed, R., Elgarøy, Ø., Dahle, H., & Keränen, P. 2004, *A&A*, 420, 1025
 204. Paczynski, B. 1990, *ApJ*, 365, L9
 205. —. 1992, *Acta Astronomica*, 42, 145
 206. Palmer, D. M. 2002, *Memorie della Societa Astronomica Italiana*, 73, 578
 207. Palmer, D. M., Barthelmy, S., Gehrels, N., et al. 2005, *Nature*, 434, 1107
 208. Pavlov, G. G., Sanwal, D., & Teter, M. A. 2004, in *IAU Symposium*, Vol. 218, *Young Neutron Stars and Their Environments*, ed. F. Camilo & B. M. Gaensler, 239–+
 209. Perna, R. & Hernquist, L. 2000, *ApJ*, 544, L57
 210. Perna, R., Hernquist, L., & Narayan, R. 2000, *ApJ*, 541, 344
 211. Pivovarov, M. J., Kaspi, V. M., & Camilo, F. 2000, *ApJ*, 535, 379
 212. Pizzolato, F., Colpi, M., De Luca, A., Mereghetti, S., & Tiengo, A. 2008, *ArXiv e-prints*, 803
 213. Popov, S. B. & Stern, B. E. 2006, *MNRAS*, 365, 885
 214. Psaltis, D. & Miller, M. C. 2002, *ApJ*, 578, 325
 215. Rea, N., Israel, G. L., Stella, L., et al. 2003, *ApJ*, 586, L65
 216. Rea, N., Nichelli, E., Israel, G. L., et al. 2007, *MNRAS*, 381, 293
 217. Rea, N., Oosterbroek, T., Zane, S., et al. 2005, *MNRAS*, 361, 710
 218. Rea, N., Testa, V., Israel, G. L., et al. 2004, *A&A*, 425, L5
 219. Rea, N., Turolla, R., Zane, S., et al. 2007, *ApJ*, 661, L65
 220. Rothschild, R. E., Kulkarni, S. R., & Lingenfelter, R. E. 1994, *Nature*, 368, 432
 221. Schwartz, S. J., Zane, S., Wilson, R. J., et al. 2005, *ApJ*, 627, L129
 222. Seward, F. D., Charles, P. A., & Smale, A. P. 1986, *ApJ*, 305, 814
 223. Stella, L., Dall’Osso, S., Israel, G. L., & Vecchio, A. 2005, *ApJ*, 634, L165
 224. Strohmayer, T. E. & Ibrahim, A. I. 2000, *ApJ*, 537, L111
 225. Strohmayer, T. E. & Watts, A. L. 2005, *ApJ*, 632, L111
 226. —. 2006, *ApJ*, 653, 593
 227. Sugizaki, M., Nagase, F., Torii, K., et al. 1997, *PASJ*, 49, L25
 228. Tam, C. R., Gavriil, F. P., Dib, R., et al. 2007, *ArXiv e-prints*, 707
 229. Tam, C. R., Kaspi, V. M., Gaensler, B. M., & Gotthelf, E. V. 2006, *ApJ*, 652, 548
 230. Tam, C. R., Kaspi, V. M., van Kerkwijk, M. H., & Durant, M. 2004, *ApJ*, 617, L53
 231. Taylor, G. B., Gelfand, J. D., Gaensler, B. M., et al. 2005, *ApJ*, 634, L93
 232. Terasawa, T., Tanaka, Y. T., Takei, Y., et al. 2005, *Nature*, 434, 1110
 233. Testa, V., Rea, N., Mignani, R. P., et al. 2007, *ArXiv e-prints*, 712
 234. Thompson, C. & Beloborodov, A. M. 2005, *ApJ*, 634, 565
 235. Thompson, C. & Duncan, R. C. 1993, *ApJ*, 408, 194
 236. —. 1995, *MNRAS*, 275, 255
 237. —. 1996, *ApJ*, 473, 322
 238. Thompson, C., Duncan, R. C., Woods, P. M., et al. 2000, *ApJ*, 543, 340
 239. Thompson, C., Lyutikov, M., & Kulkarni, S. R. 2002, *ApJ*, 574, 332
 240. Tiengo, A., Mereghetti, S., Turolla, R., et al. 2005, *A&A*, 437, 997
 241. Torii, K., Kinugasa, K., Katayama, K., Tsunemi, H., & Yamauchi, S. 1998, *ApJ*, 503, 843
 242. Usov, V. V. 1994, *ApJ*, 427, 984

-
243. van Paradijs, J., Taam, R. E., & van den Heuvel, E. P. J. 1995, *A&A*, 299, L41+
 244. Vasisht, G. & Gotthelf, E. V. 1997, *ApJ*, 486, L129+
 245. Vasisht, G., Gotthelf, E. V., Torii, K., & Gaensler, B. M. 2000, *ApJ*, 542, L49
 246. Vietri, M., Stella, L., & Israel, G. L. 2007, *ApJ*, 661, 1089
 247. Vink, J. & Kuiper, L. 2006, *MNRAS*, 370, L14
 248. Vrba, F. J., Henden, A. A., Luginbuhl, C. B., et al. 2000, *ApJ*, 533, L17
 249. Wachter, S., Patel, S. K., Kouveliotou, C., et al. 2004, *ApJ*, 615, 887
 250. Wang, Z., Bassa, C., Kaspi, V. M., Bryant, J. B., & Morrell, N. 2007, *ArXiv e-prints*, 711
 251. Wang, Z. & Chakrabarty, D. 2002, *ApJ*, 579, L33
 252. Wang, Z., Chakrabarty, D., & Kaplan, D. L. 2006, *Nature*, 440, 772
 253. Wang, Z., Kaspi, V. M., Osip, D., et al. 2006, *The Astronomer's Telegram*, 910, 1
 254. Watts, A. L. & Strohmayer, T. E. 2006, *ApJ*, 637, L117
 255. Wilson, C. A., Dieters, S., Finger, M. H., Scott, D. M., & van Paradijs, J. 1999, *ApJ*, 513, 464
 256. Woods, P. M., Kaspi, V. M., Thompson, C., et al. 2004, *ApJ*, 605, 378
 257. Woods, P. M., Kouveliotou, C., Finger, M. H., et al. 2007, *ApJ*, 654, 470
 258. Woods, P. M., Kouveliotou, C., Gavriil, F. P., et al. 2005, *ApJ*, 629, 985
 259. Woods, P. M., Kouveliotou, C., Göğüş, E., et al. 2002, *ApJ*, 576, 381
 260. Woods, P. M., Kouveliotou, C., van Paradijs, J., et al. 1999, *ApJ*, 524, L55
 261. —. 1999, *ApJ*, 519, L139
 262. Woods, P. M. & Thompson, C. 2006, *Soft gamma repeaters and anomalous X-ray pulsars: magnetar candidates (Compact stellar X-ray sources)*, 547–586
 263. Xu, R. 2007, *Advances in Space Research*, 40, 1453
 264. Xu, R. X., Tao, D. J., & Yang, Y. 2006, *MNRAS*, 373, L85
 265. Zane, S., Turolla, R., Stella, L., & Treves, A. 2001, *ApJ*, 560, 384